TECHNICAL MEMORANDUMS

NATIONAL ADVISORY COMMITTEE FOR AERONAUTICS

No. 808

HIGH-SPEED WIND TUNNELS

By J. Ackeret

Paper presented at the Fifth Convention of the Volta Congress, Italy, September 30 to October 6, 1935

Washington
November 1936

NATIONAL ADVISORY COMMITTEE FOR AERONAUTICS

TECHNICAL MEMORANDUM NO. 808

HIGH-SPEED WIND TUNNELS*

By J. Ackeret

A. PURPOSE AND GENERAL PROPERTIES OF HIGH-SPEED WIND TUNNELS

High-speed wind tunnels are of practical as well as theoretical value for the solution of certain aerodynamic problems. There exist today many applications of high velocities whose fundamental nature we understand but little. Our lack of knowledge has increased as higher and higher velocities are being used in various engineering problems as well as aeronautics and information on these high velocity applications is urgently needed.

It was in connection with the science of ballistics that the air resistance at high velocities was first investigated. To classify a velocity c as high or low, it was compared to the sound velocity a, which was thus used as a measure of the relative magnitude of a velocity.

The compressibility factor $M = \frac{c}{a}$, also known as the Mach number, serves as a criterion for the classification of wind tunnels into "subsonic" and "supersonic" tunnels, respectively. For the investigation of projectiles, only such tunnels as give supersonic velocities need be considered; investigations with small values of M being relatively unimportant. It will be an important event in the history of ballistics when it is possible to compute the path of a projectile from data obtained in the high-speed wind tunnel. It will then also be possible to investigate how the air resistance could be further reduced, the effect on the stability, etc. Certainly, very much could be learned from tests on projectiles although, as in the case of airplane tests, it is not possible to vary all the important variables independently and over a sufficient

---

*"Windkanäle für hohe Geschwindigkeiten." Publication of the Reale Accademia d'Italia. (Presented at the Fifth Convention of the Volta Congress, September 30 to October 6, 1935.)

range. Recently we have acquired much new information on steam turbines. In this connection, too, the problem of supersonic velocities enters, although this high-speed range is generally avoided - higher efficiencies being obtained at velocities well below that of sound. Aviation engineering should keep in close touch with developments in steam turbines since the exhaust turbine will acquire greater importance in the near future and it is not impossible that the gas turbine may be applied for airplane drive at high altitudes. Much useful information on flow at high velocities is also available in connection with blower construction. High-speed investigations, on the other hand, will serve as a stimulus for further development in these fields of engineering.

Up to a short time ago only propellers were considered for which M was at most equal to 1. In spite of many very important individual results obtained, many problems are still unsolved and, moreover, there exists no method of computation which satisfactorily takes into account the air compressibility. In recent times airplanes themselves have been flown at very high speeds giving considerable Mach number values. This is true not only for racing airplanes, especially designed for high speed, but also for military airplanes which may acquire unusually high velocities in dives. At these velocities the lift coefficients are quite small so that only the lower portion of the polars need be considered. Locally, however, very high velocities are set up, and these must be considered in strength computations. This problem is in some respects connected with the problem of cavitation, where the local velocities are similarly of great importance.

Since high velocities are mostly sought at high altitudes, the lowered temperature becomes a factor of importance. This lowered temperature reduces the sound velocity and thus increases the Mach number.

An accurate description of the steady flow will be characterized as a function of:

1) The Mach number

$$M = \frac{c}{a} \qquad a = \sqrt{gkRT}$$

2) The Reynolds Number

$$Re = \frac{c\,L\,\rho}{\mu}$$

3) The number of atoms of the gas characterized by the value of

$$k = \frac{c_p}{c_v}$$

If, for example, the values of M, Re, k for two geometrically similar bodies are equal, there is similarity of flow; that is, the flow lines are likewise geometrically similar. There are equal ratios between the densities, pressures, velocities, and temperatures, so that measurements on the model are sufficient to determine the actual full-scale magnitudes. The viscosity and heat-conduction coefficients must be assumed as constant within the field of flow. Practically, condition 3) denotes that the airplane-model test should also be conducted with air. In the case of steam turbines, on the other hand, it would be necessary to employ a triatomic gas for the model tests. Experience has shown, however, that for Mach numbers below 1, tests conducted with air are still useful and apparently the results may be carried over to the full-scale turbine.

We shall soon see, however, that it is very difficult to satisfy simultaneously conditions 1) and 2): $M_{mod} = M_{full\ scale}$, $Re_{mod} = Re_{full\ scale}$. In the supersonic range M will first of all be chosen equal but to attain the same Reynolds Number is very difficult even in the subsonic range. It has become customary, however, to use a smaller Reynolds Number for the model than that for the full-scale size. It is a fortunate circumstance that the differences in the data thus obtained are never very large and that they may to some extent be estimated as long as the values of the Reynolds Number are not less than certain mimimum values.

The power required for the tests may be computed as follows: We define

$$\beta = \frac{\text{kinetic energy possessed by air}}{\text{output at blower shaft}}$$

Let the test section area be F, the reference length $\sqrt{F}$; β is a function of the Mach and Reynolds Numbers for the tunnel

$$M = \frac{c}{a}; \qquad Re = \frac{c\sqrt{F}\rho}{\mu}$$

The power is:

$$L = \frac{1}{\beta}\frac{\rho}{2} c^3 F$$

$$= \frac{1}{\beta}\frac{1}{2} Re^2 M \frac{\mu^2 a}{\rho} = \frac{1}{2\beta} Re^2 M \frac{\mu^2 \sqrt{gkRT}}{\rho}$$

where all the values refer to the test section.

For μ we obtain approximately from the kinetic gas theory

$$\mu = \frac{1}{3} l \bar{c} \rho$$

Furthermore, $p = \frac{1}{3} \rho \bar{c}^2$

$$\rho = nm$$

$$l = \frac{1}{\sqrt{2\pi}\, n \sigma^2}$$

where

l is the free path of the molecules

$\bar{c}$, the mean molecular velocity

n, number of molecules per unit volume

m, mass of a molecule

σ, diameter of the molecule

Using the Avogadro law,

$$m g R = C$$

Where C is a constant (of molecular dimensions) for all gases, we obtain finally:

$$L = \left(\frac{C^{3/2}}{12\pi^{\frac{1}{2}}}\right)\left(\frac{Re^2 M}{\beta}\right)\left(\frac{\sqrt{km}}{\sigma^4}\right)\left(\frac{T^{3/2}}{\rho}\right)$$

The first parenthesis is a constant, the second depends on the properties of the tunnel desired, the third on the

nature of the gas, the fourth on the condition of the gas at the test section, chosen at will. If we assume β as constant for definite values of Re and M, then it follows that the tunnel dimensions, pressures, etc., must be so chosen that T is as low as possible while ρ is as large as possible. This means, however, that we should use cool air, with cooling before expansion at the throat, and small dimensions for the tunnel so as to work with correspondingly greater densities.

Therefore, as long as a high Reynolds Number is an important factor of consideration, the tunnel should not be built too large. This is naturally favorable from an economic point of view, but too small a tunnel is not very practical. It should be remembered, for example, that the mounting of the model at high dynamic pressures becomes difficult when the dimensions are small, since the supporting parts become relatively larger. Still more important, however, is the possibility of employing sufficiently large models in larger tunnels, especially when pressure-distribution measurements are to be taken. A solution which will satisfy all conditions is, naturally, not possible.

The theory of compressible flows is at the present time in a very favorable state of development, although it is true viscosity and heat conduction are generally left out of account. It must still be left to experiment to fill the existing gaps in our information.

B. WIND TUNNELS FOR SUBSONIC VELOCITIES

For the purposes of flight-engineering problems, it is hardly necessary at the present time to go beyond values of M = 1. Such values would also require unusually high power expenditure if the model size and the Reynolds Number are at the same time to be sufficiently large. Figure 1 shows a small tunnel that was built in Dresden according to the plans of Busemann. A centrifugal blower of about 300 horsepower provides a closed circulation of the air and produces a free 170 mm (6.7 in.) jet having a velocity approaching that of sound. A honeycomb, which is at the same time a cooler, removes the heat developed by the constant energy expenditure. Essentially the same set-up must be used for the larger constructions. On account of the strong vibrations, a fully closed construction is preferable for the

larger sizes and, furthermore, the energy expenditure and therefore also the heat that must be conducted away, are considerably smaller for this type of construction. The compressibility of the air creates new problems in design. The velocity along most of the stream path is still very small and the losses at the bends, for example, are known from previous experience. The pitot-tube pressure, however, is no longer given accurately by $\frac{\rho}{2} c^2$ but is larger, according to the formula:

$$\Delta p_{pitot} = \frac{\rho}{2} c^2 \left\{1 + \frac{1}{4} M^2 + \frac{2-k}{24} M^4 + \ldots\right\}$$

The temperature T along the test portion (which theoretically should be measured with a thermometer that is moved along) is lower than that behind the chamber T_o and is given by the formula:

$$\frac{Ac^2}{2g} = c_p (T_o - T) = c_p \Delta T$$

Figure 2 serves as an example. Let the air at a temperature 300° C. issue from a very large space into a space having a pressure of 10,000 kg/m². Using the values $k = 1.4$, $c_p = 0.24$, $R = 29.28$, $A = \frac{1}{427}$, the curves of figure 2 are obtained showing the ratio $\frac{\rho}{2} \frac{c^2}{\Delta p_{pitot}}$ plotted against the velocity c. To determine the velocity, it is necessary to know the pressure and temperature at the chamber and the outside pressure.

For the absolute pressures and densities, we have the well-known adiabatic relations:

$$\frac{p}{p_o} = \left(\frac{T}{T_o}\right)^{\frac{k}{k-1}} ; \quad \frac{\rho}{\rho_o} = \left(\frac{T}{T_o}\right)^{\frac{1}{k-1}}$$

The closed test portion of the tunnel must be carefully adjusted, especially on account of the increasing boundary layer at the higher velocities through the narrowed section. If we denote any cross section area by f then from the equation of continuity:

$$\frac{f\ c}{v} = \text{constant}$$

we obtain $$\frac{df}{f} + \frac{dc}{c} - \frac{dv}{v} = 0$$

For the velocity, we have:

$$\frac{c\,dc}{g} = - v\ dp$$

or $$\frac{dc}{c} = - \frac{g\ v\ dp}{c^2}$$

The flow is very nearly adiabatic, so that

$$p\ v^k = \text{constant}$$

or $$\frac{dp}{p} + k\ \frac{dv}{v} = 0$$

and therefore, $$\frac{df}{f} - \frac{g\ v\ dp}{c^2} + \frac{1}{k}\ \frac{dp}{p} = 0$$

$$\frac{df}{f} = \frac{g\ p\ v}{c^2}\ \frac{dp}{p} - \frac{1}{k}\ \frac{dp}{p}$$

Using the relations $a^2 = g\ k\ p\ v$ and $M = \frac{c}{a}$, we finally obtain:

$$\frac{dp}{p} = \frac{k\ M^2}{1 - M^2}\ \frac{df}{f}$$

In the neighborhood of the velocity of sound, therefore, the slightest change in cross section is accompanied by a very large change in pressure, making measurements with a closed tunnel very difficult if the walls of the former are not adjustable. But even for the open jet, difficulties are encountered when $M = 1$.

Figure 3 shows a test arrangement for the study of the pressures and efficiencies in a high velocity test chamber with connected diffuser or exit cone. Figure 4 is a photograph of the entire installation. The air was delivered by an axial type compressor (maximum output 500 horsepower) was straightened by a honeycomb and flowed

through the cylindrical test portion (7.88" 200 mm) and the adjoining sheet-metal cone out into the atmosphere. The pressures were measured at the points noted on the figure, and thermocouples were used to measure the inlet temperature. The obstacle shown at the side of the figure could be introduced into the test section. The tests were mainly intended to give information on the restored pressure efficiency of the cone at the higher Mach numbers. Figure 5 shows the measured pressure distribution with the obstacle removed. While there is no appreciable pressure drop along the test portion at low velocities, the pressure drop increases very much in the neighborhood of the sound velocity in agreement with the explanation given above. The effect of the exit cone or diffuser may be characterized by an exit cone efficiency η_d. In the case of incompressible flow η_d is given by the pressure rise that is produced. With compressible flows several definitions are possible. If we consider the entropy diagram (fig. 6), we have an expansion from the pressure p_o to p_1 at the test section, with increase in velocity. The diffuser recovers the pressure p_2. The efficiency on the basis of pressure is

$$\eta_{pres} = \frac{p_2 - p_1}{p_o - p_1}$$

The energy expenditure required for producing the air flow or, more properly, for covering the losses is not, however, determined by the above formula, since $1 - \eta_{pres}$ does not accurately represent the energy loss. L. Crocco, in his very important study on high-speed wind tunnels, defines the exit-cone efficiency in such a way that for an infinitesimal increase in pressure, as for the case where compressibility is not considered, he writes:

$$\eta_d \frac{c\, dc}{g} = - v\, dp$$

For the time being η_d may be assumed constant throughout the compression and the state of the gas represented on the entropy diagram.

According to the energy theorem,

$$i + A \frac{c^2}{2g} = \text{constant}$$

(the exchange of heat with the surroundings being neg-

lected) $\eta_d \, di = A \, v \, dp$. The entropy equation

$$dS = \frac{c_v \, dT}{T} + \frac{A \, p \, dv}{T}$$

and the gas equation then easily lead to the conclusion that the element of energy loss $(1 - \eta_d) \, A \, \frac{c \, dc}{g}$ in heat units is given by the cross-hatched element of area $T \, dS$. It follows, furthermore, that with constant η_d the curve becomes even steeper, since for equal increases in temperature the area representing the energy loss must increase correspondingly, and at a higher temperature dS is smaller. The energy loss area (fig. 6 II) is not, however, equal to the work that must be expended by a blower of the usual construction. This would require a very definite expansion process and special cooling. Practically what happens is that the air is taken up by the blower after it goes through the diffuser and in the ideal case is adiabatically compressed (fig. 6 III). After compression the temperature T' is reached and the amount of heat $c_p (T' - T_o)$ per kilogram; that is, the cross-hatched area must be removed. This loss is naturally greater than that shown in figure 6 II. It may be asked what is the best condition that could be attained from the thermodynamical viewpoint. Figure 6 IV shows another process which is, however, only of theoretical interest. Let the lowest cooling water temperature available be T_w. The air behind the exit cone is assumed to flow first through a turbine which does an amount of work $c_p (T_o - T_w)$ per kilogram, then follows an isothermal compression with cooled blower and finally an adiabatic compression to p_o which again raises the work of the turbine. The amount of work expended is equal to the cross-hatched area, which is somewhat less than the previous one. Only the case corresponding to the third diagram must be considered in practice. The difference between the efficiency on the basis of pressure and that on the basis of energy loss from figure 6 III is shown in figure 7 for a Mach number of 0.6 corresponding to a velocity of about 200 meters per second. We define

$$\eta_{pres} = \frac{p_2 - p_1}{p_o - p_1}$$

$$\eta_{energy} = 1 - \frac{T' - T_o}{T_o - T_1}$$

so that η_{energy} is somewhat larger than η_{pres}.

The pressure distribution (fig. 5) shows the rise in pressure expected when the sound velocity at the exit-cone entrance is exceeded and when the pressure is partly produced by a compression impulse.

The corresponding energy efficiency is computed according to figure 6 III, compensating for the kinetic energy of the mean velocity at the end of the exit cone. Figure 8 shows a constant value of 0.85 for the efficiency up to the neighborhood of the sound velocity. For $M = 0.94$ there is a decrease, which means practically that it is not possible to raise the velocity at the measuring section by a further decrease in the pressure at the end of the exit cone, and from this we learn that the cross sections at supersonic velocities must be essentially of different form. From the curve we may obtain the important result that a restoring of pressure up to $M = 1$ is possible with normal exit cones. Figure 9 shows the entropy diagram for two points corresponding to $M = 0.584$ and $M = 0.77$.

For small values of M the obstacle introduced does not change the normal pressure distribution (fig. 10). There is, however, an increased sensitivity in the pressure changes with cross-section changes, especially in the neighborhood of the sound velocity, since the cross section at the narrowest portion changes when the test body is introduced. It is possible that a free jet in the neighborhood of $M = 1$ would offer some advantages as far as ease of measurement is concerned, but we have made no tests on this point. An interesting phenomenon was the strong, shrill noise that was noted as the velocity of sound was approached.

When the amount of the pressure restored by the exit cone is known, the tunnel propeller can be designed. Pressure differences of from 500 to 1,000 kg/m^2 may be obtained with a good arrangement, so that single-stage blowers may be used up to tunnel velocities of 200 meters per second (450 miles per hour). The peripheral velocity of the propeller is limited by considerations of strength and the velocity of sound. A further limit to the pressure difference produced, is the separation of the flow at the innermost parts of the blades. This necessitates thicker hubs which decrease the propeller cross section and raise the velocity of the air passing through the pro-

peller by such a large amount that additional losses are produced.

We define the following nondimensional magnitudes:

$$\psi = \frac{\Delta p}{\frac{\rho}{2} u^2} \qquad \varphi = \frac{c_{ax}}{u}$$

$$\nu = \frac{\text{hub diameter}}{\text{outside diameter}}$$

and further, $\sigma = \varphi^{1/2} \psi^{-3/4} (1 - \nu^2)^{1/2}$

which factor is a good index for the type of blower used.

If we desire full output at the hub, it is necessary for the blade width and the peripheral velocity to be sufficiently large. Figure 11 shows the hub to propeller diameter ratio as a function of ψ for different values of the product c_a blade width per blade separation.

At smaller pressures - that is, at high velocities, it is possible to work with a smaller output, since in that case the rise of pressure through the propeller occurs at the expense of the kinetic energy. At higher pressures (smaller σ) this is no longer possible since the kinetic energy is smaller compared to the pressure rise produced at the wheel. The decreased energy at the hub in the first case must naturally be made up later, either by turbulence in the exit cone or by throttling at the faster moving parts.

Apparently, therefore, a bigger hub is of advantage. Experiments have shown that also for a smaller hub construction, a rather big hole is torn in the energy curve and this is mainly on account of the insufficient turbulence when the walls are fixed. De Tomasi set up a diffuser arrangement with a throttling insert that permits the air passing through it to be throttled down to zero. Strange to say, full closure gives a better pressure recovery than a small outflow, and this is probably due to the fact that the mixing tendency is greater in the first case (fig. 12). The upper limit for the peripheral velocity, not considering the strength requirements, is limited by the circumstance that as the velocity of sound is approached, the profile drag increases at the higher lifts

and separation sets in even at the small lifts. It is therefore necessary first, to keep the relative velocity below a certain limit; and second, to work with a low value of c - that is, use large blade widths. Assuming that the highest local velocity is to be 0.9 times the velocity of sound, figure 13 is obtained for the limits of the peripheral velocity. These values still remain to be tested experimentally, although they are probably too high rather than too low. For example, with $\psi = 0.4$ and the large overlap ratio of 0.75, a peripheral velocity of 260 meters per second is still permissible and the corresponding pressure difference produced is 1,690 kg/m^2. Such values have already been obtained in practice. It is important to remember that the pressure restored by the exit cone varies with the object of the test that is being conducted, and a reserve is necessary. With single-stage wheels the pressure can hardly exceed 1,000 mm W.S. (1/10 atmosphere).

Up to a short time ago, it was not possible to obtain the high efficiencies that were theoretically expected at high pressures. Whereas the wheel (fig. 14) still gives good efficiencies, namely, $\eta = 0.84$ at $\psi = 0.2$ (including the losses in the exit cone behind the wheel); the high-pressure wheel (fig. 15) gives a considerably lower efficiency, $\eta = 0.77$ at $\psi = 0.5$. In these tests the loss at the hub is eliminated by placing a cylindrical tube behind the hub. Otherwise, the difference would be still greater.

Separation at the blades occurred not so much between the blades as at the edges between the blades and the wall (fig. 16). The design of the blade ends as shown in figure 17 improved the performance somewhat, although the polars for the set of blades still showed large losses compared to that of the single blade (fig. 18). The maximum lift is here determined by the separation at the rim.

In our tests with the tunnel propellers, it was possible to give the air an adjustable spiral movement before reaching the propeller. At higher values of ψ a system of guide vanes is indispensable since the spiral motion is considerable and would be a great source of disturbance. Guides placed in front of the wheel have the advantage that the air is strongly accelerated and enters the wheel very smoothly. This improves the efficiency and reduces the noise. With the guide behind the wheel there is the advantage that the air leaves the blower without spiral motion, but under certain conditions there are considerable losses at the guide vanes.

In recent times the propeller blades have been designed so that their setting is adjustable, thus making it possible to control the velocity to a large extent. The driving motor does not then require a very large velocity range but only certain discrete velocities. Figure 19 shows the blower characteristics using variable blade settings. With fixed blade the spiral motion of the air can less easily be regulated (fig. 20). When the resistances vary a great deal, as, for example, when using nozzles of different diameters, it is absolutely necessary for the blades to be adjustable. Figure 21 shows how it is possible to handle masses of air of quite different volumes with good efficiency. Adjustable blades are also important for variable density tunnels because they make possible full output within a large range.

In closed high-speed tunnels, it is necessary to remove the heat into which the propeller output is converted. It is well known that in order to obtain a good relation between the heat conducted away and the loss in pressure, it is necessary that the cooler be placed at a section where the velocity is small, since the heat conduction increases with the velocity to a power that is less than 1. It is, obviously, advantageous to construct the honeycomb so that it acts as a cooler at the same time, whereby the advantage of a very good smoothing out of the velocities greatly outweighs the somewhat increased pressure loss. Such coolers are also very useful for tunnels where tests on air-cooled engines are to be conducted.

The blower drive may be designed as is customary at the present time, and I shall not enter into this question except to point out a method that will probably be applied in the future and which will give very high performance, namely, steam drive using Velox boilers. Full output of the propeller is rarely used, relatively speaking, and therefore the fact that the turbine efficiency is somewhat smaller at full load than at small loads, is not of great importance. The usual power turbines are not to be taken as examples. There are surprising possibilities of improved performance within a small range. An example will make this clearer. A closed iron tunnel is designed for a maximum velocity of 700 km/h (435 miles per hour) and having a diameter of 4.5 meters at the test section. The tunnel is also to be operated at a vacuum and with pressures above atmospheric - in the latter case at reduced velocity. The tunnel is to operate with the best efficiency possible on account of the small power output and

amount of cooling, and therefore small-angle cones and large cross sections for the cooler must be used. Figure 22 shows a section through the tunnel. The propeller has adjustable blades, a diameter of 7.5 meters, and a maximum speed of 600 r.p.m.

The tunnel may be operated at a vacuum or at pressures up to 10 atmospheres. By adjusting the blades it is possible at this latter pressure to operate at a velocity of 300 km/h (about 190 miles per hour).

A wing of 3-meter span and 50 centimeters mean chord could be investigated in the first case at a Reynolds Number of 6.8×10^6 and a Mach number of 0.57. In the second case $M = 0.245$ and Re increases to 29×10^6. By evacuating the tunnel M could be raised somewhat. In such tunnels considerable difficulty is met with in supporting the models and obtaining the corresponding forces for the full-scale wing or airplane.

The turbines (two housings) (fig. 23) work at a speed of 4,800 r.p.m. and are adjusted to the speed of the propeller. It is possible to obtain a maximum output of 25,000 horsepower with good efficiency. The flow of the steam takes place at an unusually high velocity but it is possible by means of the diffuser to recover a considerable portion of the pressure and to work with a vacuum in the condenser of 0.08 atmosphere.

The chief obstacle to the application of steam was, until now, the inconvenience in placing the boiler and especially, the long time required to start up the turbine and the poor regulation possible, due to the large quantities of heat stored up in the brickwork, etc. This has all been changed now at one stroke. The B.B.C Velox boiler whose development is founded largely on the recent progress made in aerodynamics does all, so to speak, that is reasonably required of a wind-tunnel drive. The boiler takes up very little space and requires no special attention. Even very powerful units may, within 10 minutes, be brought up from the cold condition to full pressure. The efficiency is unusually high, 93 percent being repeatedly obtained in tests with only a slight decrease at part load. The boiler adjusts itself to load changes almost instantly. Since it could be operated with fuel oil, the fuel cost per horsepower-hour is not larger than for the Diesel engine. The chief new feature of the Velox steam generator is the possibility of combustion under higher pressure and the

burned gases therefore possess considerable velocity. This makes possible very good heat conduction, which fact leads to small dimensions and small amount of water necessary. The compression of the combustion gases consumes only a small amount of the power which is now supplied by the gas turbine operating on the exhaust gases of the boiler. With increasing efficiency of the compressor and turbine, there is possible also an increase in the furnace pressure which, in the present constructions, amounts to about 2 to 3 atmospheres.

Figure 24 shows a cross section through the boiler, figure 25, a view of the whole arrangement, and figure 26, the results on tests showing the unusually high efficiencies at part load. Figure 27, finally, is a diagram of a starting-up test showing the minimum time required for heating up the boiler.

C. SUPERSONIC TUNNELS

If it is desired to attain velocities approaching those met with in ballistics, the problem of energy becomes of even greater importance. For the solution of the problem, the following methods are available:

a) Using the energy from an air reservoir for short time intervals during the test and storing up the air during the remainder of the time.

b) Operating the tunnel continuously with a vacuum, in which case the Reynolds Number will be less in proportion to the pressure.

Both of these methods have their advantages and disadvantages. By method a), it is difficult to carry out tests involving heat conduction but high Reynolds Numbers are relatively easy to obtain. By method b) the reverse is true. Figures 28 and 29 show schematically the arrangement for the stored-up method of operation with direct drive. The high-speed wind tunnel at Göttingen, for example, consists of two vacuum tanks into which the air from the outside enters after passing through the experimental chamber. A quick-closing cock cuts off the air from the tank. The air may be taken from the atmosphere - with the disadvantage, however, that there is a possibility of ice formation on the models. The installation at

Göttingen, therefore, uses dried air from an air tank (fig. 28, bottom). Figure 29 shows another arrangement with the above method of operation, at only subsonic velocities, however, and is the one used at the N.A.C.A. and N.P.L. The high-pressure air is taken from large tanks that surround the high-pressure tunnel. From the point of view of economy, direct operation with high-pressure air would be more advantageous, but it has the disadvantage, however, that the pressure and temperature change during the test. A pressure regulator would remove the first disadvantage, but the temperature would still fall since any throttling process would have no effect on it. In this case, too, special means must be provided against the tendency toward ice formation. The time intervals required for the tests with the arrangement of figure 28 may easily be computed from a knowledge of the fact that a constant weight must flow through the minimum cross section during the test interval, neglecting the exchange of heat with the walls.

Let the volume of the air container be V m^3, the specific weight of the container γ_i; $i = c_p T_i$ equals the heat content per kilogram. If the amount of air flowing through the throat per second is m, then

$$V \, d\gamma_i = m \, dt$$

The change in the energy content is

$$V \, c_v \, d(\gamma_i \, T_i) = m \, dt \left(c_v \, T_a + A \frac{p_a}{\gamma_a} \right) = m \, dt \, c_p \, T_a$$

where the index a refers to the condition of the air entering the container (at practically zero velocity).

Now

$$c_v \, T_a + A \frac{p_a}{\gamma_a} = i_a$$

which, according to the energy theorem, is equal to the heat content of the outside air:

$$i_o = c_p \, T_o$$

We thus obtain:

$$d\gamma_i = \frac{m}{V} \, dt$$

$$\gamma_i = \gamma_{i_1} + \frac{m}{V} \, t$$

Furthermore,

$$d(\gamma_i T_i) = \frac{c_p \, m \, T_o}{c_v \, V} dt$$

$$(\gamma_i T_i) = (\gamma_i T_i)_1 + \frac{m}{V} k T_o t$$

Since $$p_i = \gamma_i R T_i$$

it follows that $$\frac{p_i}{R} = \frac{p_{i_1}}{R} + \frac{m}{V} k T_o t$$

and $$p_i = p_{i_1} + \frac{m}{V} k R T_o t; \quad t = \frac{V (p_i - p_{i_1})}{m \, k \, R T_o}$$

The time interval for the test is thus directly proportional to the volume of the container and to the pressure difference that must arise in the container or tank in order that there be no disturbance in the air condition at the test section. This back pressure depends on the effectiveness of the exit cone behind the test section in restoring the pressure. Busemann states that for M = 1.47 the pressure in the tank should rise from 0.5 to 0.7 atmosphere. The air expands from 1 atmosphere to 0.284 atmosphere, and from there it rises to a maximum of 0.7 atmosphere. These figures are in good agreement with the results obtained in our tests. Figure 31 shows the pressure along the tunnel for different throats and at different Mach numbers. The diffuser, as we know, must first narrow down and then diverge. The lower diagram gives us the required pressure ratios in which other resistances at the honeycombs, bends, etc., must be included. Since the test intervals are measured in seconds even when large reservoirs are used, it is necessary to have the air cut-off occur as quickly as possible. At the Gottingen tunnel a turncock is used (fig. 32), which is started with high-pressure air and is turned in fractions of a second by means of a servomotor using oil damping. In the open setting the resistance that it offers to the flow is almost negligible.

With the continuous operation method (fig. 30), the compressor performance also depends on the restored pressure in the exit cone. The output and the Reynolds Number are proportional to the absolute pressure, which may easily be varied by means of a vacuum pump. The cooler is a new feature. The sketch on figure 30 shows how the high-

est velocities are obtained at the Zurich tunnel. One part of the compressor air is branched off after cooling and employed to drive an ejector. With the remainder of the air it is possible to attain higher velocities, since a higher pressure range is possible. The ejector serves also as an auxiliary outlet when small air masses are used as, for example, in tests on pipes. The closed arrangement has the advantage that within certain limits the Reynolds Number may be changed independently of the Mach number. This is especially important at the small Reynolds Numbers since, for these, the profile drag depends to a rather large extent on the Reynolds Number, and we still know hardly anything about the effect of compressibility on separation and turbulence. Furthermore, it is then entirely possible to work with other gases, for example, CO_2 (triatomic) or argon (monatomic).

A possible disadvantage that may be offered by the employ of such expensive gases as argon, is the lack of airtightness of the entire air passage and blower. In actual operation it was noted, however, that the leakage was quite small even with the usual method employed to gain tightness, and by using special methods such as soldering over individual flanges with thin sheet metal, etc., the airtightness could be even further improved.

It is a characteristic feature of supersonic wind tunnels that the throat, test chamber, and exit cone must be of an adjustable cross section if it is desired to have a continuous variation of the velocity. This is a matter of considerable difficulty and makes it necessary to employ rectangular forms for the tunnel, such that two opposite walls are fixed while the other two are capable of being moved. Dr. Gasperi proposed three plane walls with one adjustable wall, this symmetrical construction then corresponding to the three axial reference planes. This would have the advantage of cheaper construction and convenience in observation at the third side (fig. 33).

The test section itself must be made variable, although it should be noted that for a sufficiently steep pressure-volume characteristic the variation is small. The narrowest cross section becomes smaller at the higher Mach numbers, but the ratio:

$$\frac{\text{test section area}}{\text{minimum throat section area}} = \frac{F}{F^*}$$

becomes greater, so that there is almost compensation. With the closed tunnel arrangement, the heat exchange with the surroundings may, to a first approximation, be neglected. Then (fig. 34) $T_o = T_1$. Since $v_o = RT_o/p_o$, the weight of air per second taken up by the compressor, is

$$G = \frac{V_o\, p_o}{R\, T_o}$$

where V_o is the volume drawn in by the compressor in cubic meters per second. It is known, on the other hand, that for Laval nozzles the ratios of the pressures, temperatures, and densities in front of the nozzle and at the minimum section (denoted by *) are constant; that is,

$$\frac{T^*}{T_1};\ \frac{p^*}{p_1};\ \frac{v^*}{v}$$

are constant. G is also equal to $\frac{F^*\, a^*}{v^*}$, and moreover, $v^* = \frac{RT^*}{p^*}$ so that $\frac{V_o\, p_o}{R\, T_o} = \frac{F^*\, a^*\, p^*}{R\, T^*}$ and $F^* = \frac{V_o\, p_o\, T^*}{a^*\, p^*\, T_o} =$ const. $V_o \frac{p_o}{p_1}$. Using the pressure ratio $\vartheta = \frac{p_1}{p_o}$. We therefore obtain $F^* = \text{const.} \frac{V_o}{\vartheta}$

As may have been expected, F^* is smaller the larger the value of ϑ; that is, the larger the Mach number.

The ratio F/F^* is given by the theory of the Laval nozzle, and figure 35 shows the relation for air. If this curve is combined with that of figure 31 (bottom) which gives us the pressure ratio ϑ, it is then possible to compute the area of the test section F from the $\vartheta - V_o$ relation. We obtain the result that the curve $\vartheta - V_o$ must be rather steep, so that the propeller should show very little variation in the volume of air drawn in. This condition which otherwise is of no advantage, is very well fulfilled by the new multistage axial compressors. Figure 36 gives a comparison of the characteristics of the radial and axial compressors.

The throat should be of such a form that it permits a parallel flow at constant speed. Fortunately the charac-

teristics provide us with a good graphical method for obtaining the form of the test section for different values of M (fig. 37). Figure 38 shows different forms. The walls must therefore be designed so as to be flexible. Broad steel bands are put around the test portion, and by means of screws and links the test portion may be varied in a regular manner. Airtightness is secured by having rubber pressed against the sides. Behind the band there is the vacuum and therefore the force is not particularly strong. The band thickness is not constant but greater at the fastening points, so as not to obtain any positions on the contour having too large a curvature. The greatest variation is at the narrowest cross section. The test cross section may be left constant. The exit cone is to be constructed in the same manner as the throat. Tests show, however, that the minimum section of the cone must be larger. This is to be ascribed mostly to the boundary layer formed at the walls. The flow is naturally very complicated when the waves starting out from the body under investigation create new disturbances in the exit cone. The exit cone, too, must be capable of adjustment.

A special problem arises when the velocity to be measured is only a little above the velocity of sound. The waves strike the walls or the free jets and are reflected in the same or opposite phase. If $M \longrightarrow 1$ the reflected waves strike the test body and falsify the results - under some conditions, by a considerable amount. In two dimensional problems there is a way out by using a somewhat tedious step-by-step approximation method for curving the walls (fig. 39). It is then also possible to investigate very large bodies.

An important element is the cooler. Where is it most advantageous to place it? In front of or behind the test chamber? If it is placed in front, it receives the hot air from the blower and cools it to about room temperature. During the expansion, very low temperatures are reached; on the walls, however, on account of the friction, the temperature is almost the same as the initial temperature. The compensation is not complete, observations showing a decrease in the wall temperature. If the cooler is placed behind the test chamber, the walls are hot. It is then to be noted that the cooler in this case must have considerably larger dimensions. The fall in temperature is unchanged but the air density is less, the exit cone being able to restore only a fractional part of the original pressure. It is easy to see that the heat

conductivity for equal flow velocity is smaller. The heat exchanged increases as $(\rho c)^{0.6}$ (see fig. 40, showing test results on cooling plates) while the pressure decreases to a higher power than 1 with the velocity, so that

$$\Delta p \sim \rho^{0.6} c^{1.6}$$

If we assume, for example, the density behind the test chamber as 1/3, then for equal cooling surface c must become three times as great in order to remove the same amount of heat. This requires, however, that Δp become greater in the ratio $\left(\frac{1}{3}\right)^{0.6} \times (3)^{1.6}$; that is, three times as great. It will therefore be necessary to have the cooler larger. Another important question is the simultaneous application as a honeycomb and velocity equalizer. The velocity distribution at the outlet of the blower is, generally speaking, not sufficiently uniform. If a body, permitting the air to flow through it, is placed in the way of the flow like our cooler, then there results a very uniform distribution of the velocities. For these reasons we have decided to set up the cooler at the Zurich tunnel in front of the throat.

Axial compressors are at present being greatly developed. Figure 41 shows the characteristics of the compressor used at Zurich tunnel for different rotational speeds with the maximum number of stages. It was possible to raise the adiabatic efficiency to above 80 percent. Figure 42 shows a section through the supersonic wind tunnel at Zurich. The tunnel is so designed that the test section is approximately a square 40 by 40 centimeters, and a velocity twice that of sound can be attained. The 13-stage B.B.C. axial compressor draws in the air, for example, at 0.125 atmosphere and compresses it to 0.275 atmosphere. The rotational speed required for this is 3,500 r.p.m., and the volume drawn in about 45 cubic meters per second. For this an output of 700 kilowatts is required of the d.-c. motor. The temperature of the air brought in may rise to 45° C., the final compression temperature to 165°. Figure 43 shows the blower, which has a drum rotor. The guide-vane rims may easily be removed so that it is possible to operate with a reduced pressure ratio at a somewhat lowered efficiency. Special measures must be taken against the infiltration of outside air and to see that no oil vapor gets into the circulation. Figure 44

shows the oil circulation. The air pressure at the places requiring tightness is so maintained that the sealing oil and oil vapor are pressed toward the outside. Oil and air are then separated through filter and overflow and then return, so that neither oil nor air is lost. The saving of the gas is naturally of particular importance in operation with expensive gases. After going through the blower, the air enters the cooler (fig. 45). It consists of three rectangular elements connected, one behind the other, with vertical pipes through which the water flows, and soldered on horizontally are thin copper plates, each element being capable of being separately disconnected. The cooling ribs of the first two cooling elements are spirally wound and the last has accurately horizontal plates to direct the flow. It would be of some advantage to streamline the cooling tubes (fig. 46), although the high cooling water pressure and the expense involved in the construction kept us from doing this. The resistance is not particularly large - at full velocity being 90 mm W.S. (0.0090 atmosphere). The principle of opposed water flow is used and the water inlet and outlet pipes are so arranged that all parts of the air flowing through are cooled as uniformly as possible in order to avoid the formation of "schlieren." The pipe line is soldered out of sheet metal 5 mm thick with reinforcement against buckling. An extension is now being made so that air turbine tests could be made (fig. 47). A part of the air delivered is led through the turbine while the remainder goes through a bypass, and by the ejector effect helps to increase the pressure ratio. Figure 48 shows the rotor of the compressor; figure 49, a cooler element with flat plates; figure 50 shows one with spirally wound ribs.

Translation by S. Reiss,
National Advisory Committee
for Aeronautics.

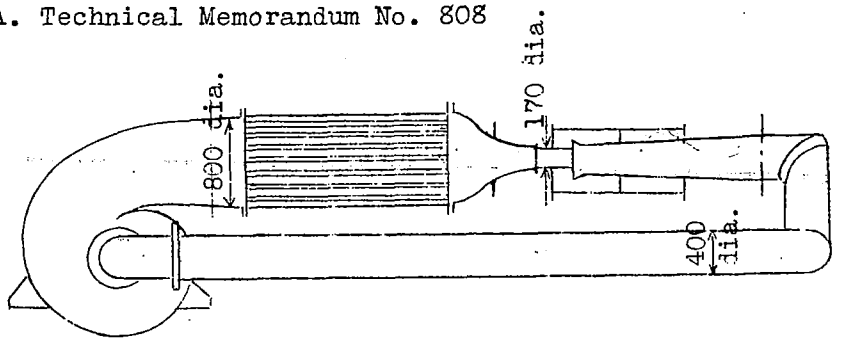

Figure 1.- Wind tunnel at the machine laboratory at Dresden.

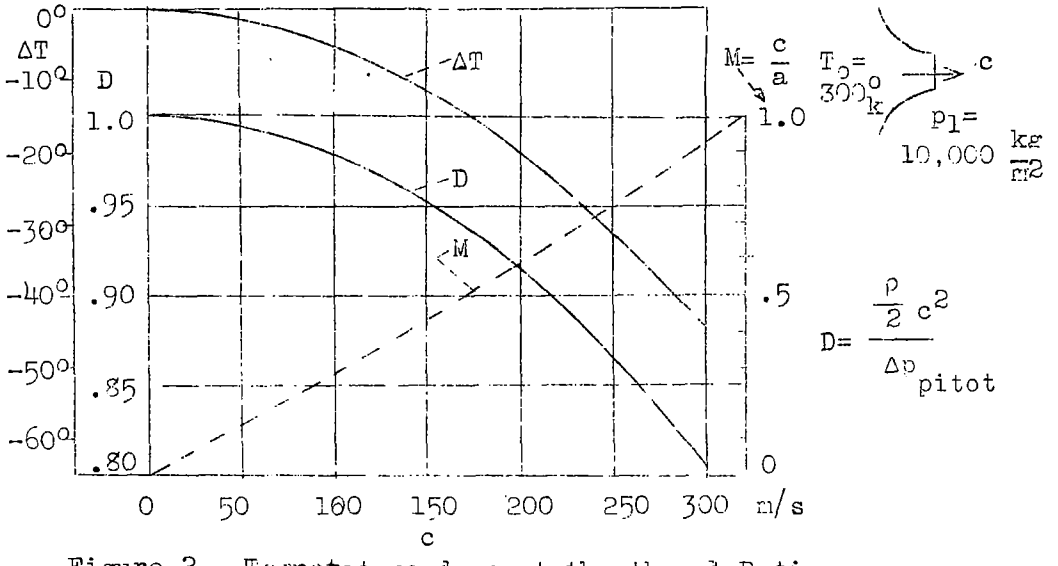

Figure 2.- Temperature drop at the throat. Ratio of pitot pressure to $\rho/2c^2$.

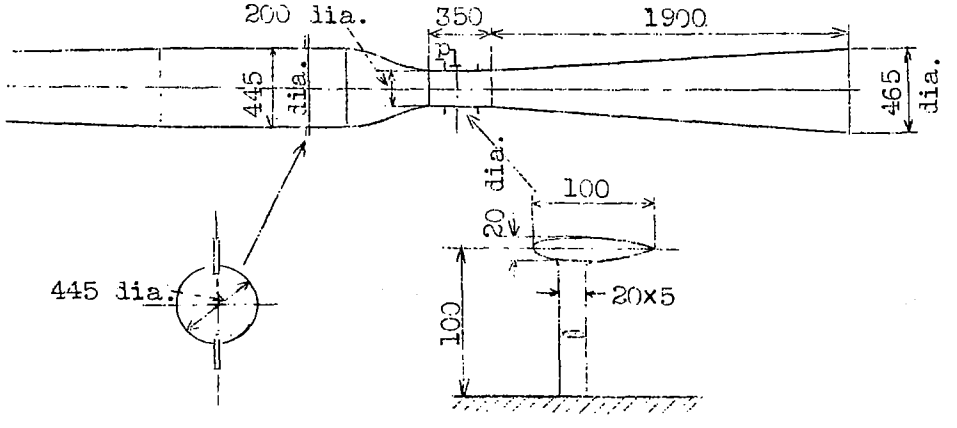

Figure 3.- Test arrangement to determine the efficiency of the diffuser or exit cone for subsonic velocities. To the right is shown body used as obstacle.

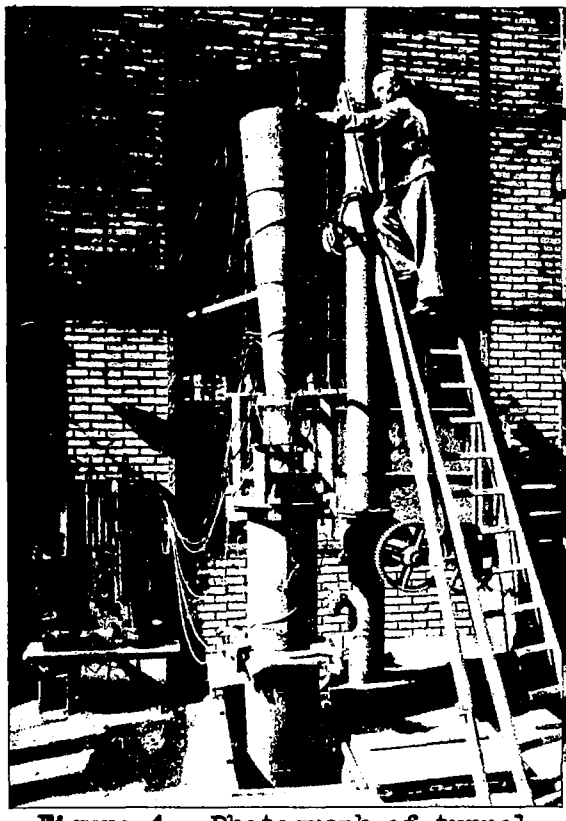

Figure 4.- Photograph of tunnel.

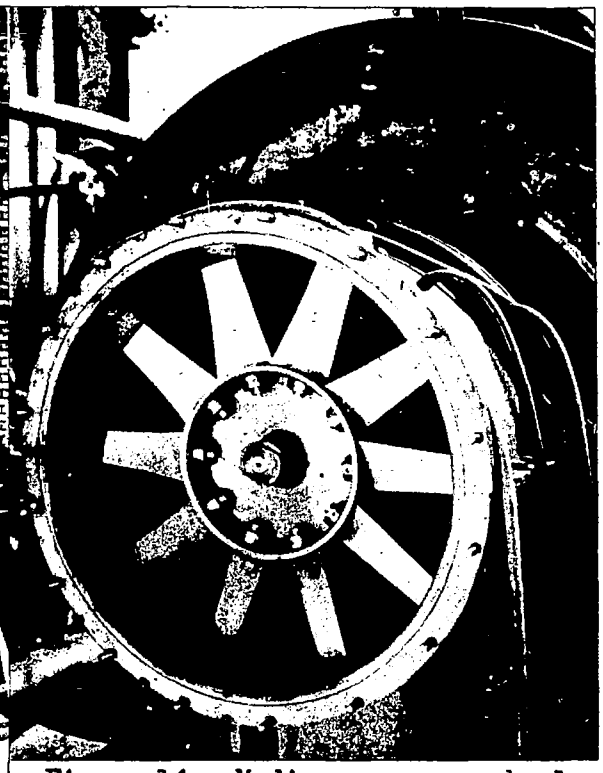

Figure 14.- Medium-pressure wheel with 10 blades $\nu = 0.47$.

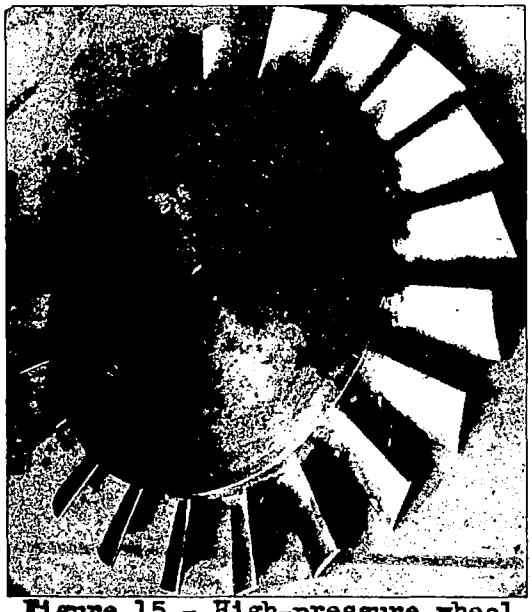

Figure 15.- High-pressure wheel with 20 blades $\nu = 0.70$.

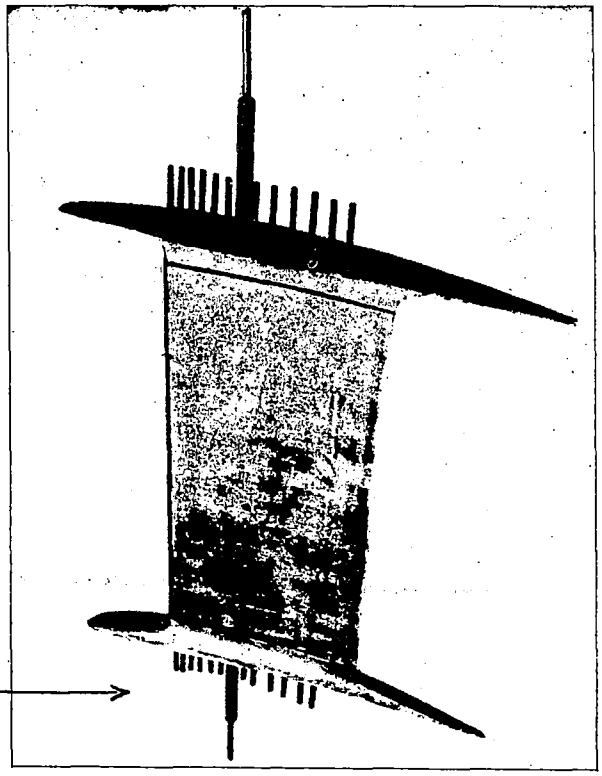

Figure 17.- Blade with end streamlining to prevent wall separation.

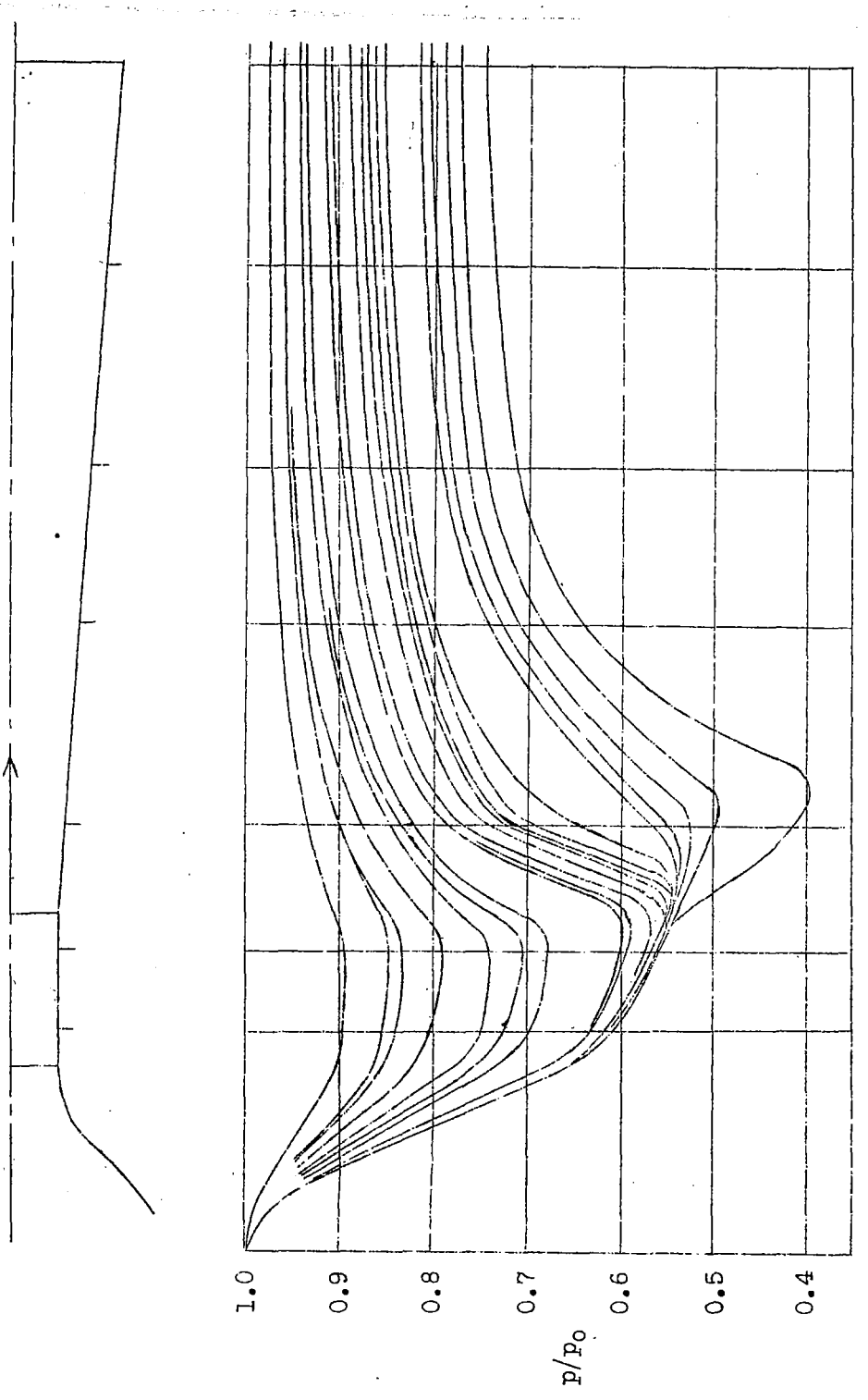

Figure 5.- Pressure distribution in the empty tunnel referred to the static pressure p_o.

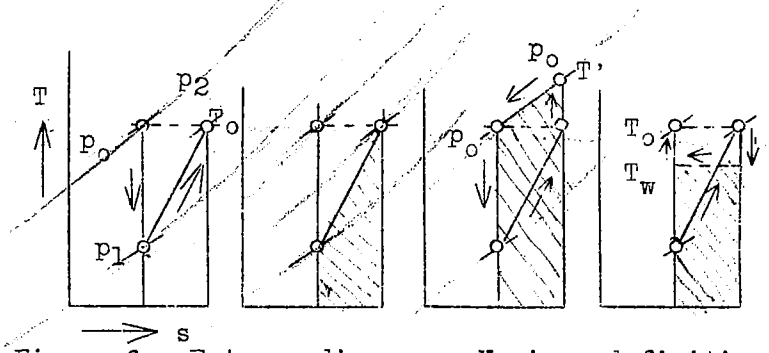

Figure 6.- Entropy diagrams. Various definitions of exit cone efficiencies.

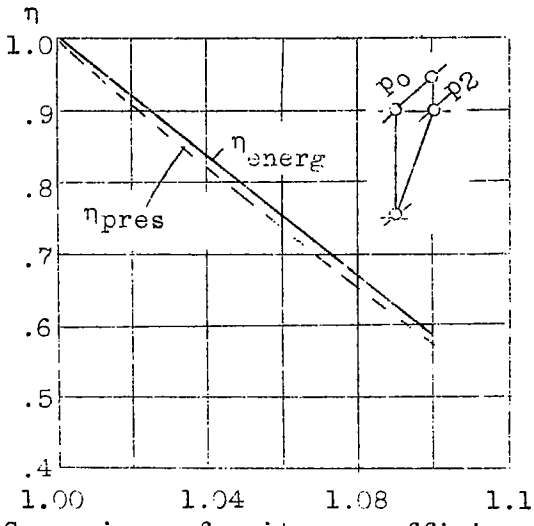

Figure 7.- Comparison of exit cone efficiency based on pressure with that based on energy.

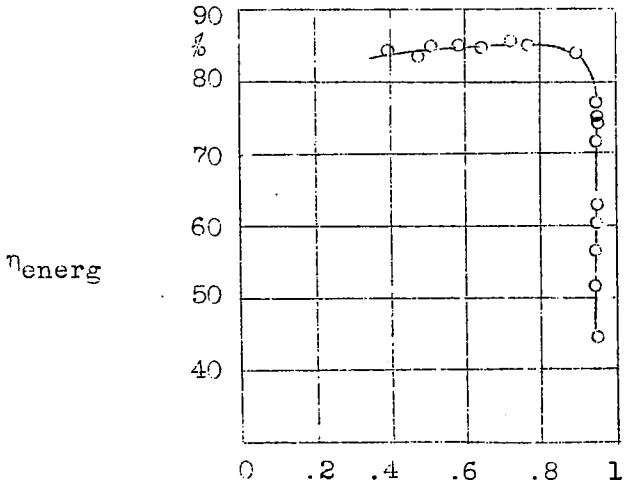

Figure 8.- Energy efficiency as a function of the Mach number.

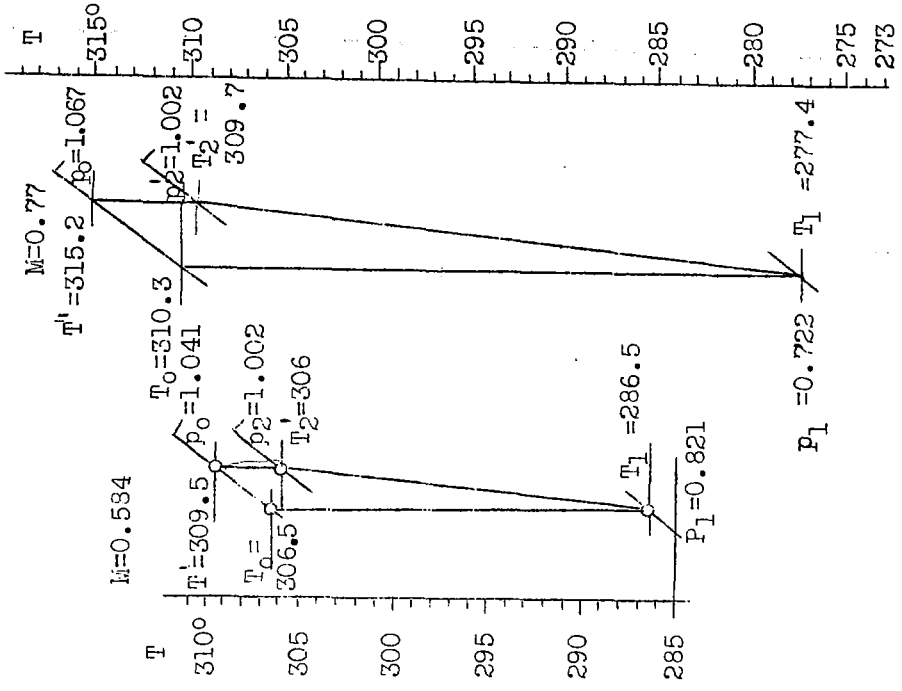

Figure 9.- Entropy diagrams for the Mach numbers M = 0.584 and M = 0.77 .

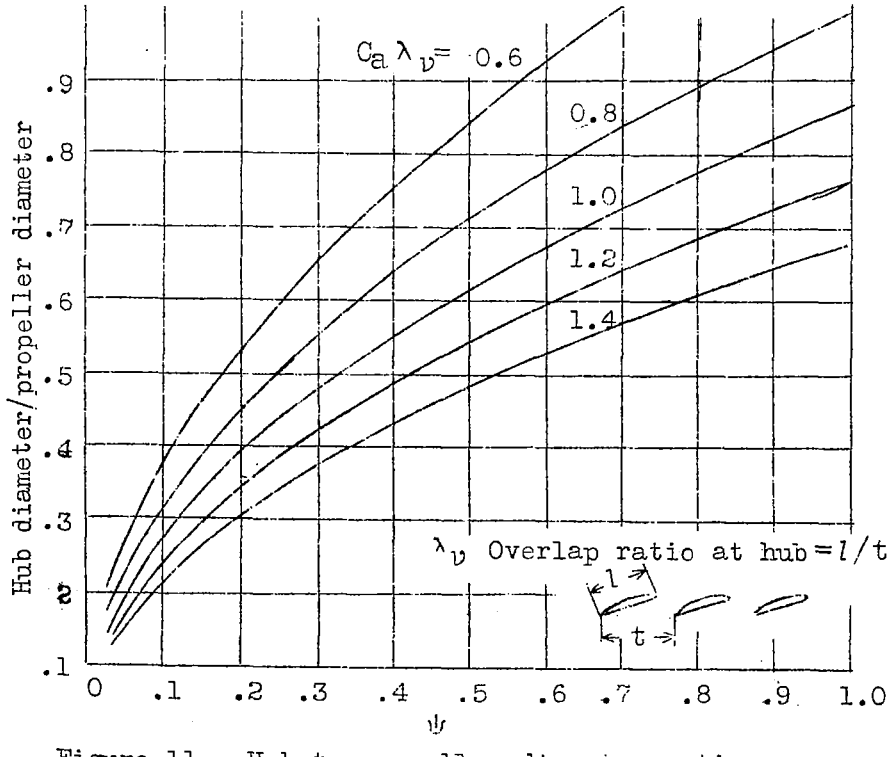

Figure 11.- Hub to propeller diameter ratio as a function of ψ .

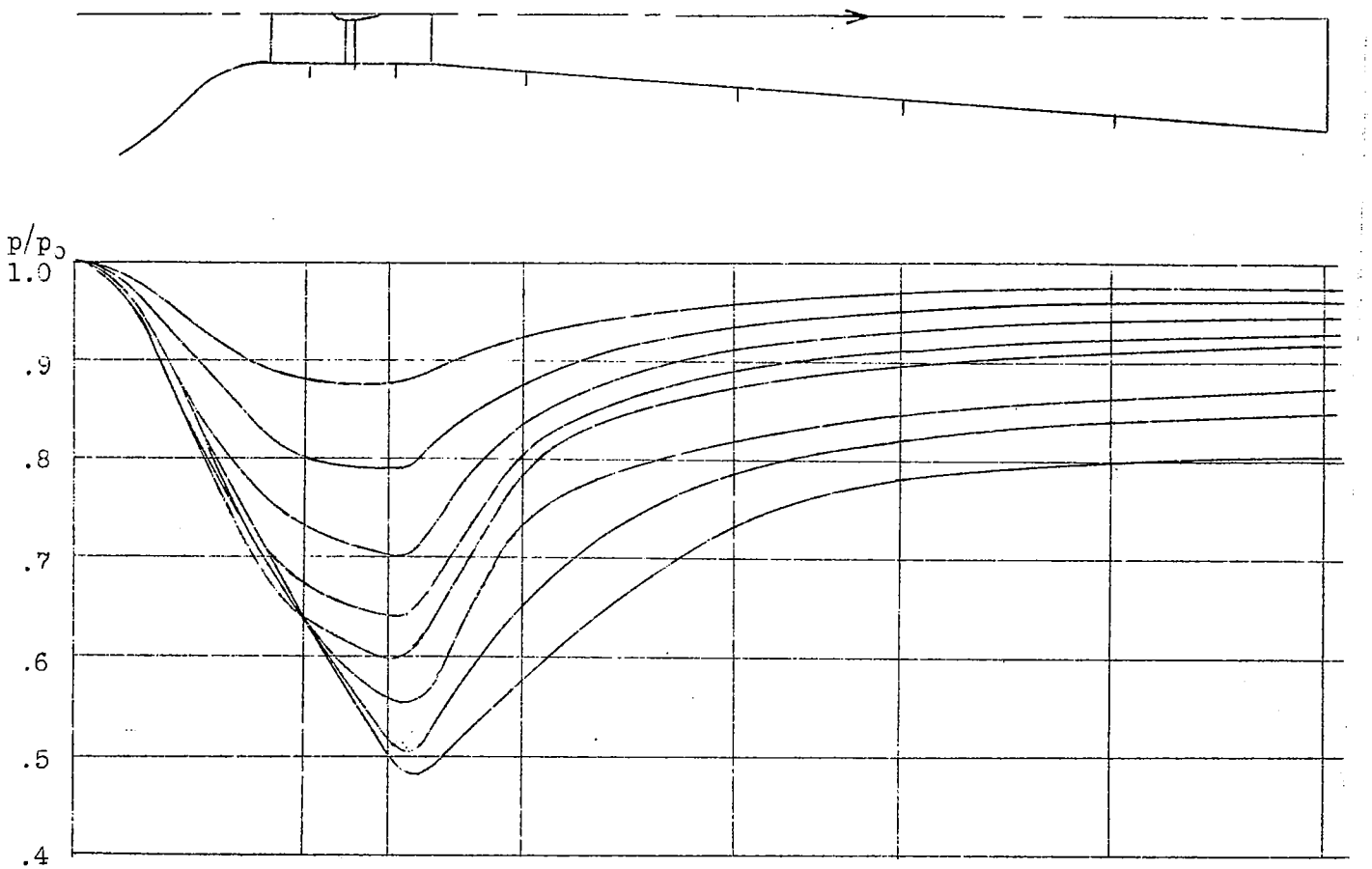

Figure 10.- Pressure distribution with obstacle present.

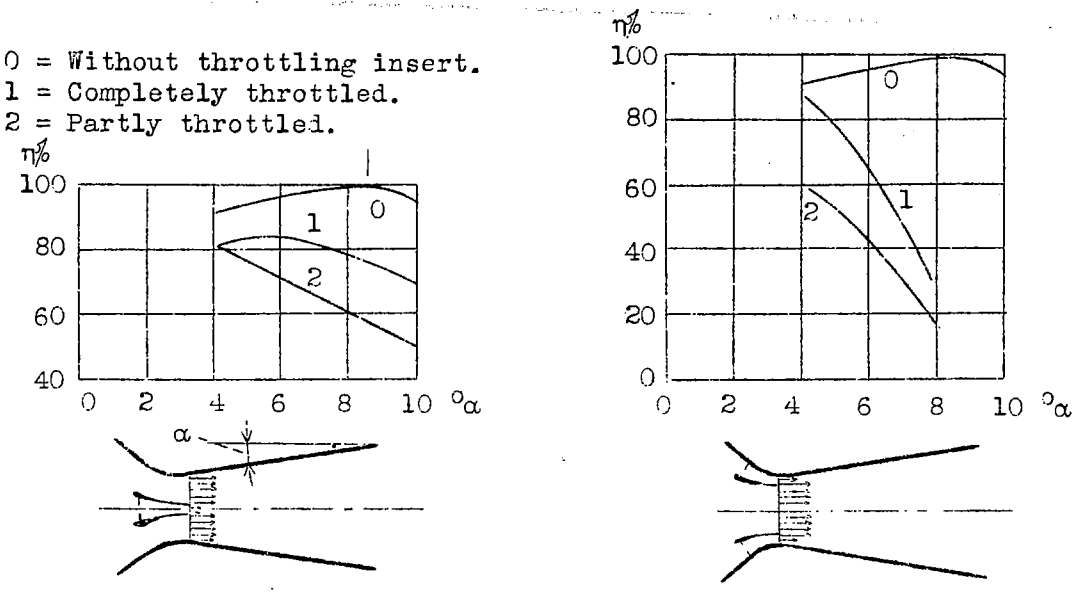

Figure 12.- Effect of throttling insert on the exit cone efficiency.

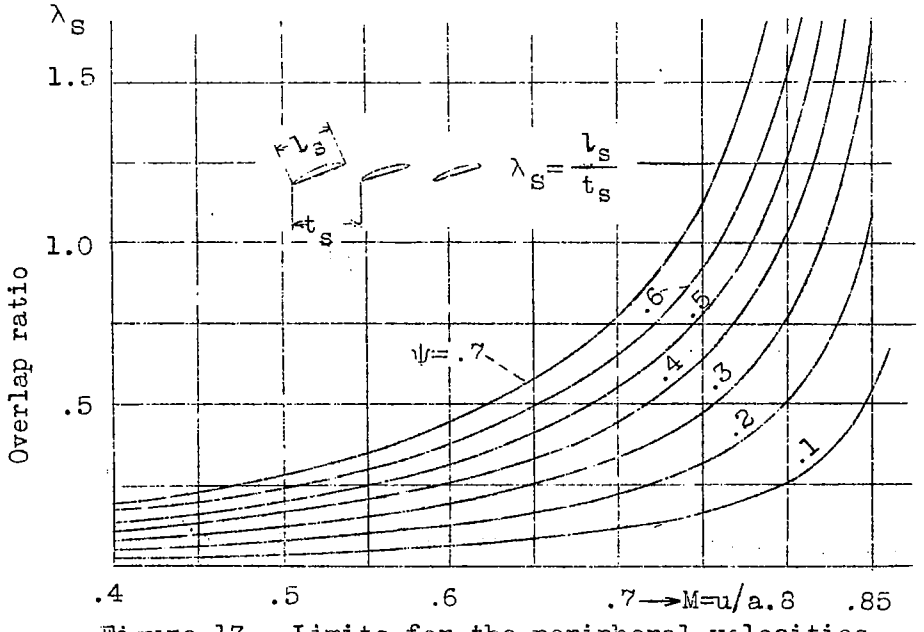

Figure 13.- Limits for the peripheral velocities determined by the compressibility.

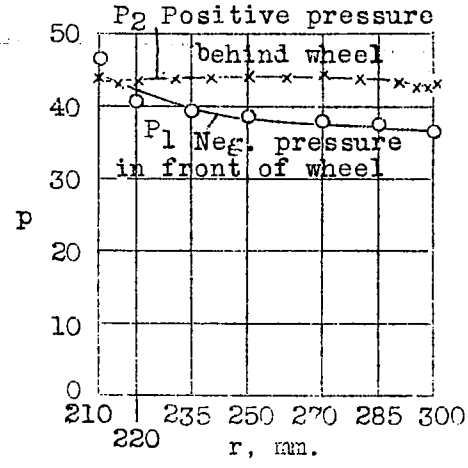

Figure 16.(continued below.)

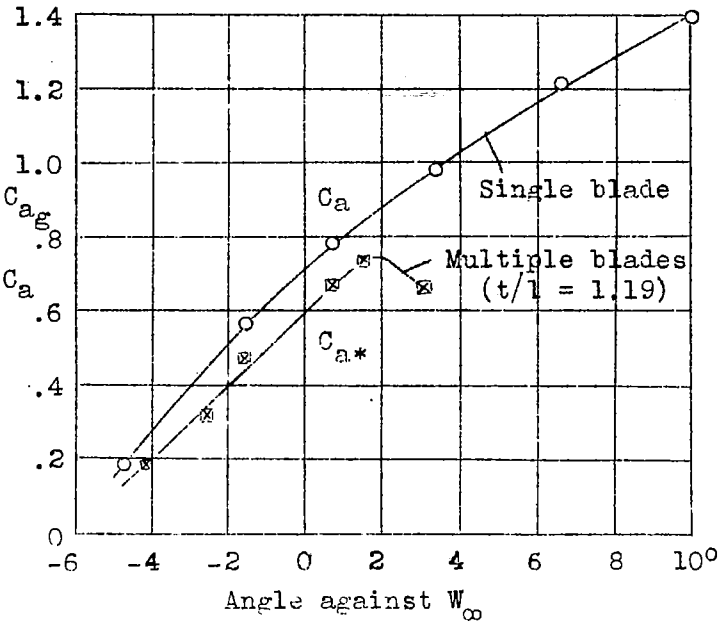

⊠ Multiple blades(Impuls)
○ Single blade (Impuls)
× Single blade (Wägung)

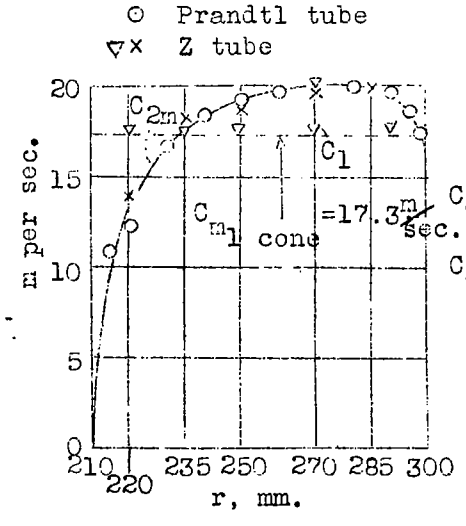

Figure 16.- Pressure and velocity distribution in front of and behind the high-pressure wheel.

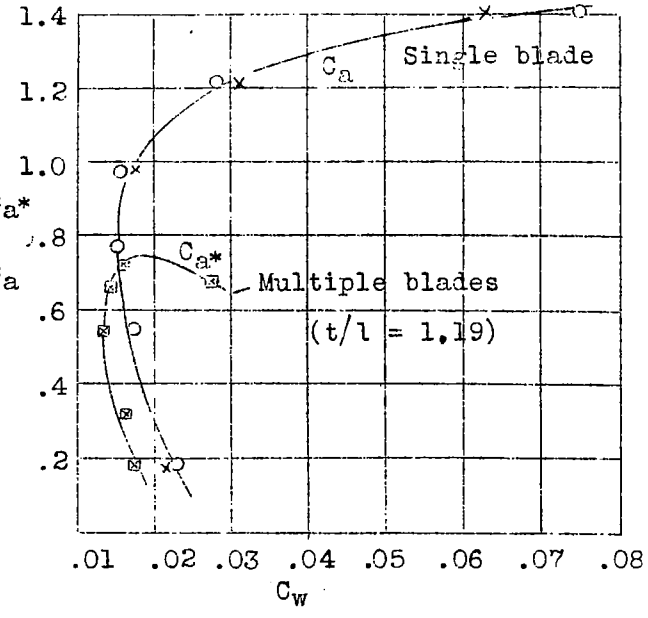

Figure 18.- Polars of single blades and multiple blades compared.

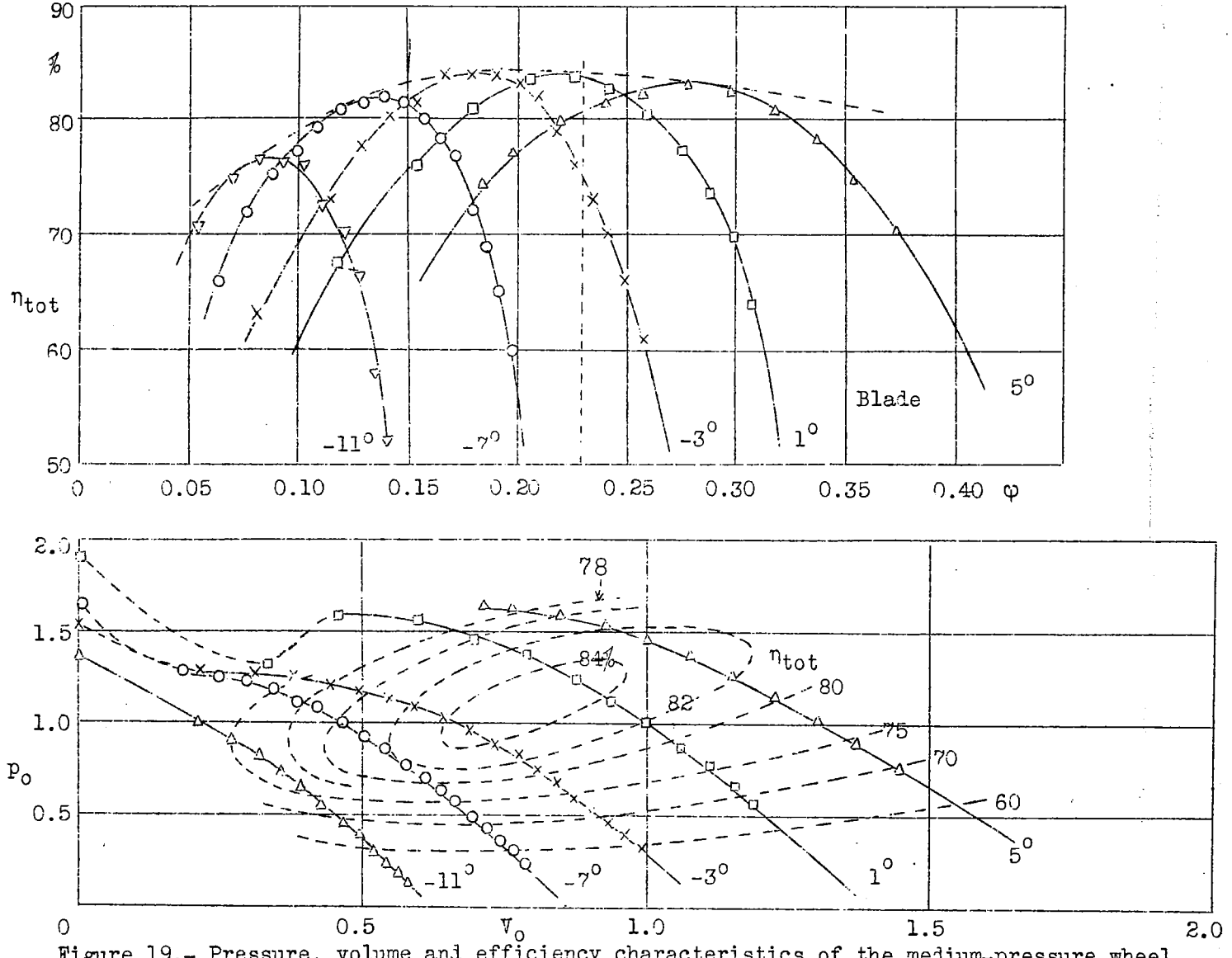

Figure 19.- Pressure, volume and efficiency characteristics of the medium-pressure wheel shown on figure 14, for different blade settings.

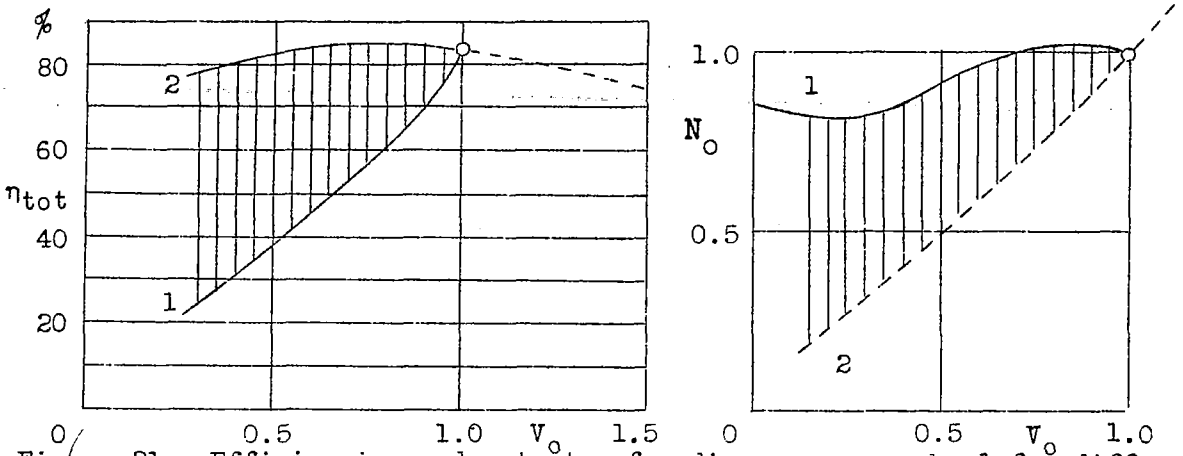

Figure 21.- Efficiencies and outputs of medium-pressure wheel for different volumes of air discharged at constant pressure., (1) Without wheel regulation. (2) with wheel regulation.

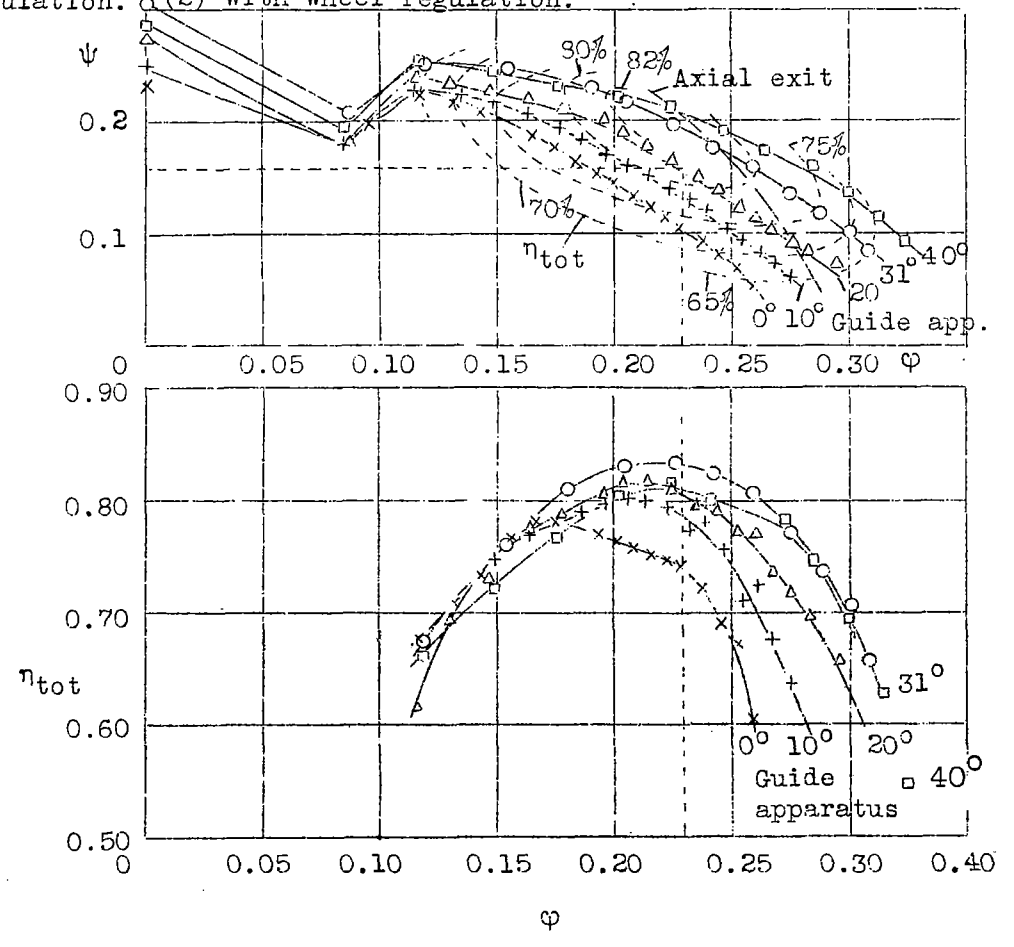

Figure 20.- Characteristics of the wheel (fig. 14) with blades held fast and spiral twist of air varied.

m	Feet
4.5	= 14.76
7.5	= 24.61

m	ft.
8.0	= 26.25
10.0	= 32.81
13.6	= 44.62

m	ft.
15.0	= 49.21
16.0	= 52.49
29.5	= 96.78
50.0	= 164.04
72.0	= 236.22

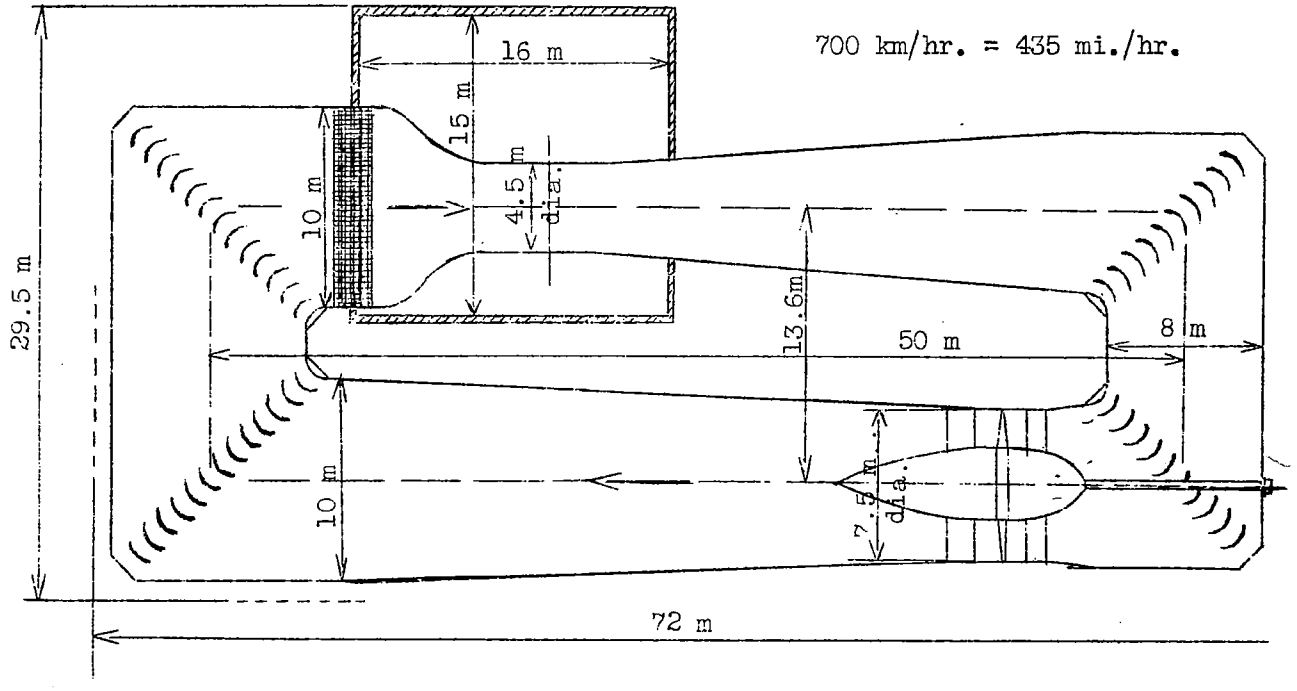

Figure 22.- Design of a high-speed wind tunnel with steam turbine drive. Throat diameter 4.5 m. Maximum velocity at atmospheric pressure at the test section 700 km/hr.

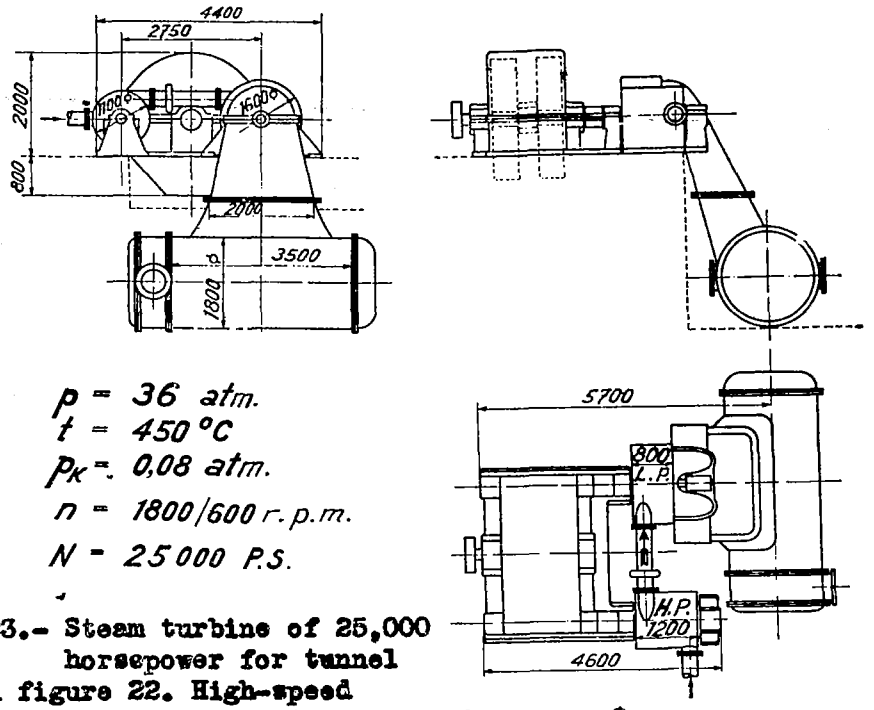

$p = 36$ atm.
$t = 450$ °C
$p_K = 0{,}08$ atm.
$n = 1800/600$ r.p.m.
$N = 25\,000$ P.S.

Figure 23.- Steam turbine of 25,000 horsepower for tunnel shown on figure 22. High-speed turbine with gear drive and Velox boiler.

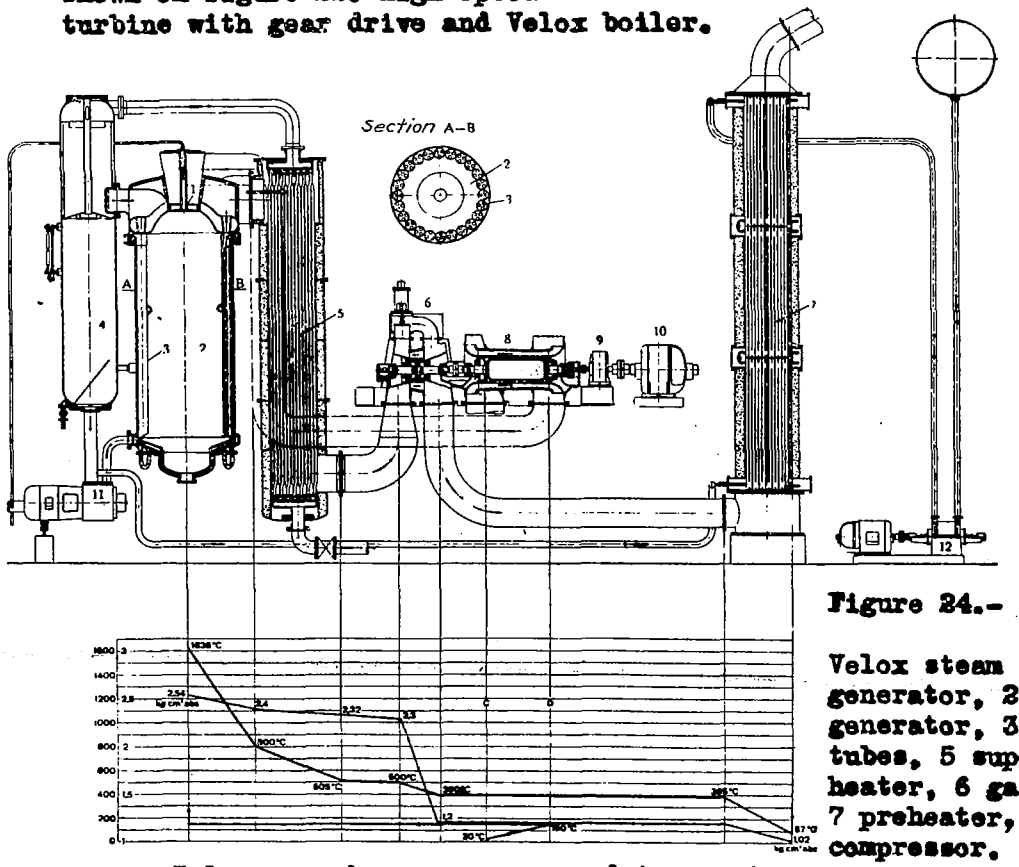

Figure 24.- Section through Velox steam generator, 2 steam generator, 3 boiler tubes, 5 superheater, 6 gas turbine, 7 preheater, 8 axial compressor.

Below are shown pressure and temperature curves.

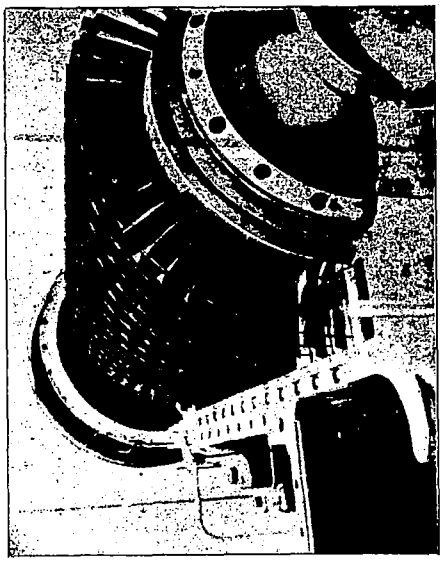

Figure 48.- Rotor of the compressor.

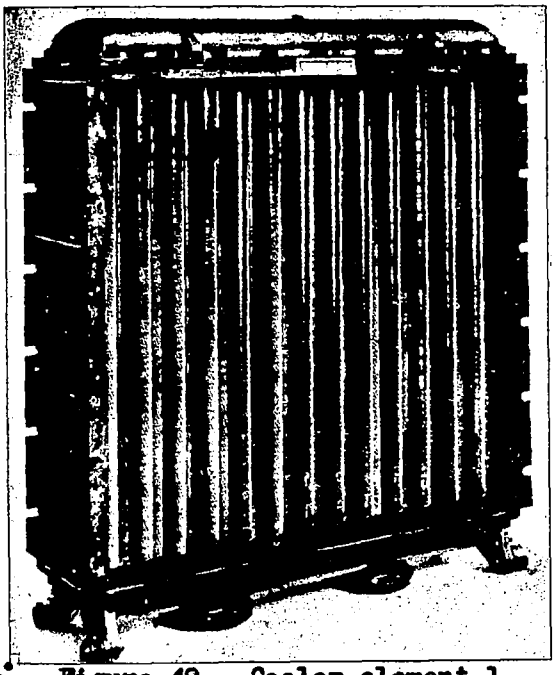

Figure 49.- Cooler element 1.

Figure 25.- Showing installation of Velox steam generator.

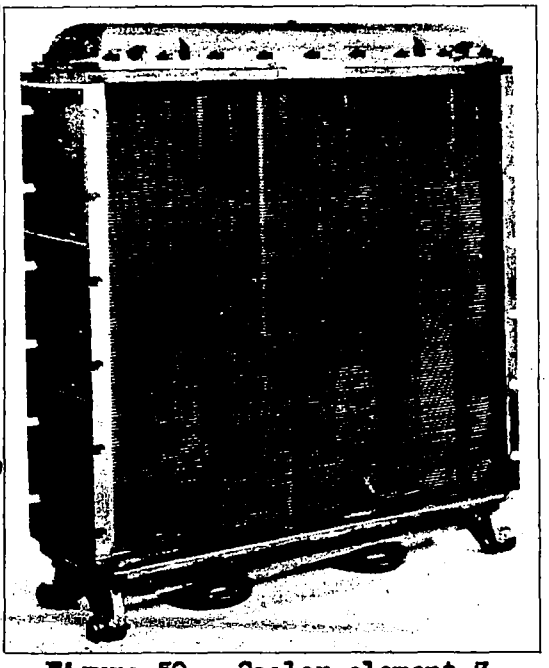

Figure 50.- Cooler element 3.

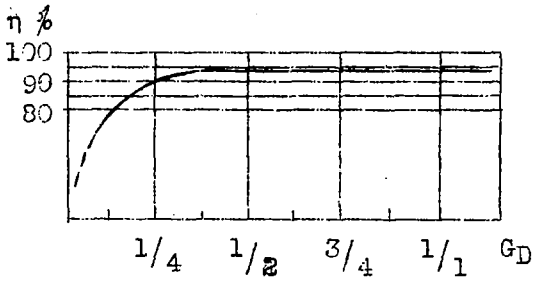

Figure 26.- Measured efficiency of Velox boiler as a function of the load.

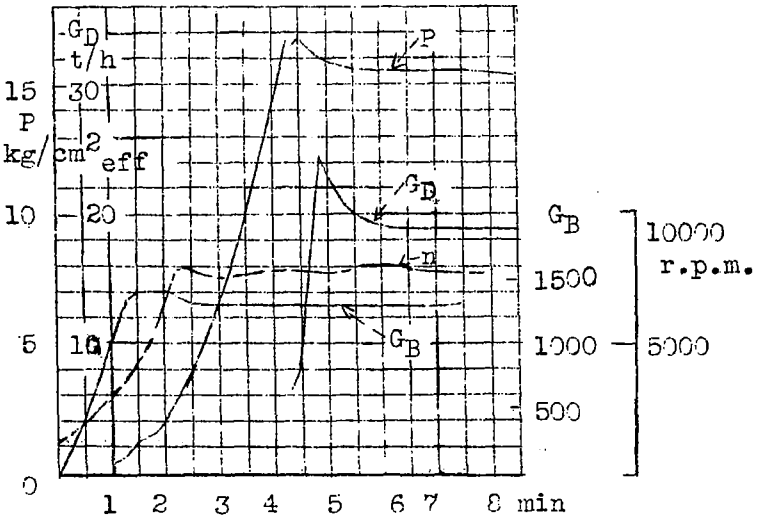

Figure 27.- Generating steam from the cold condition with a Velox boiler.

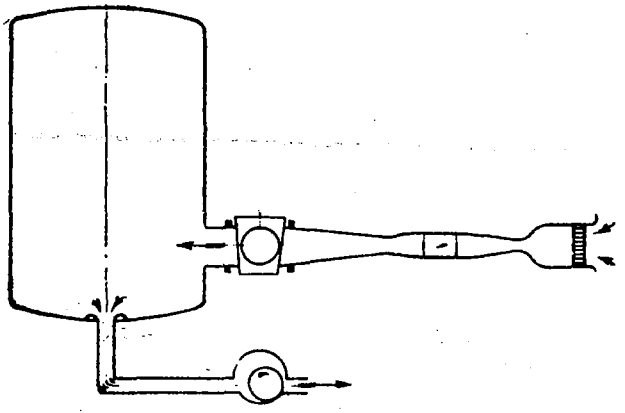

Figure 28.- Operation of supersonic tunnels with stored-up air. Above, with air taken from the test chamber, below, with dried air taken from a gasometer.

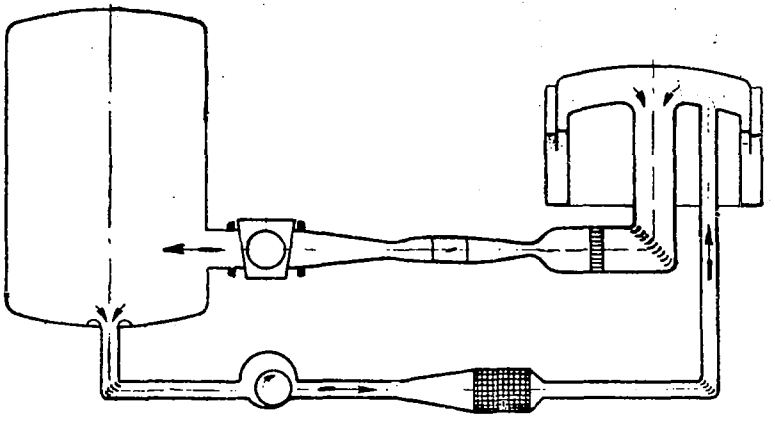

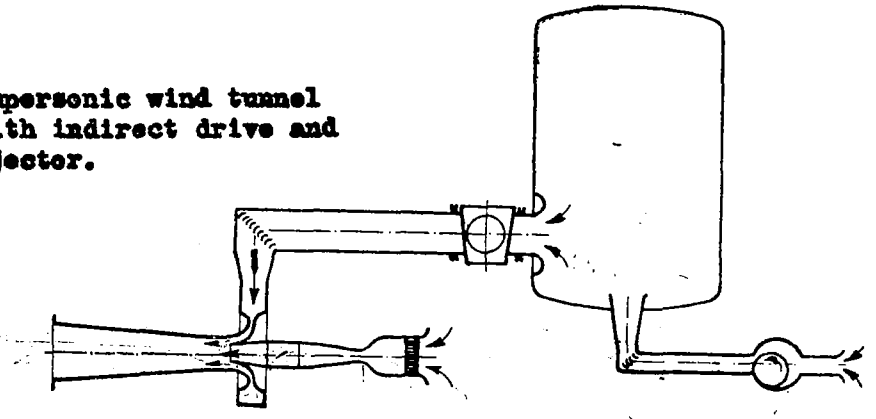

Figure 29.- Supersonic wind tunnel with indirect drive and ejector.

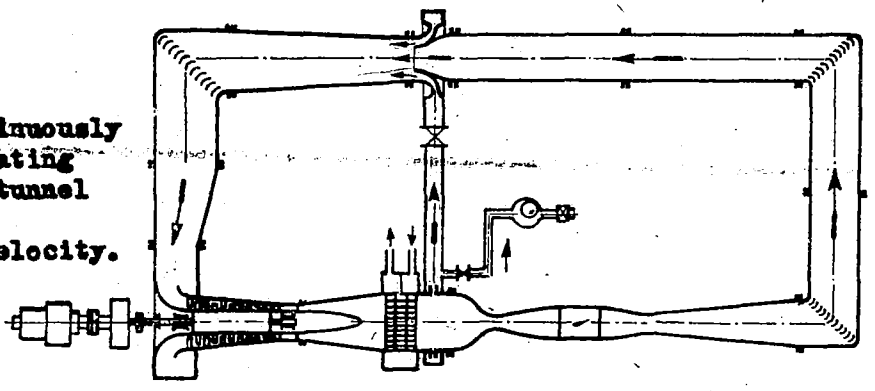

Figure 30.- Continuously operating supersonic wind tunnel with ejector for increasing the velocity.

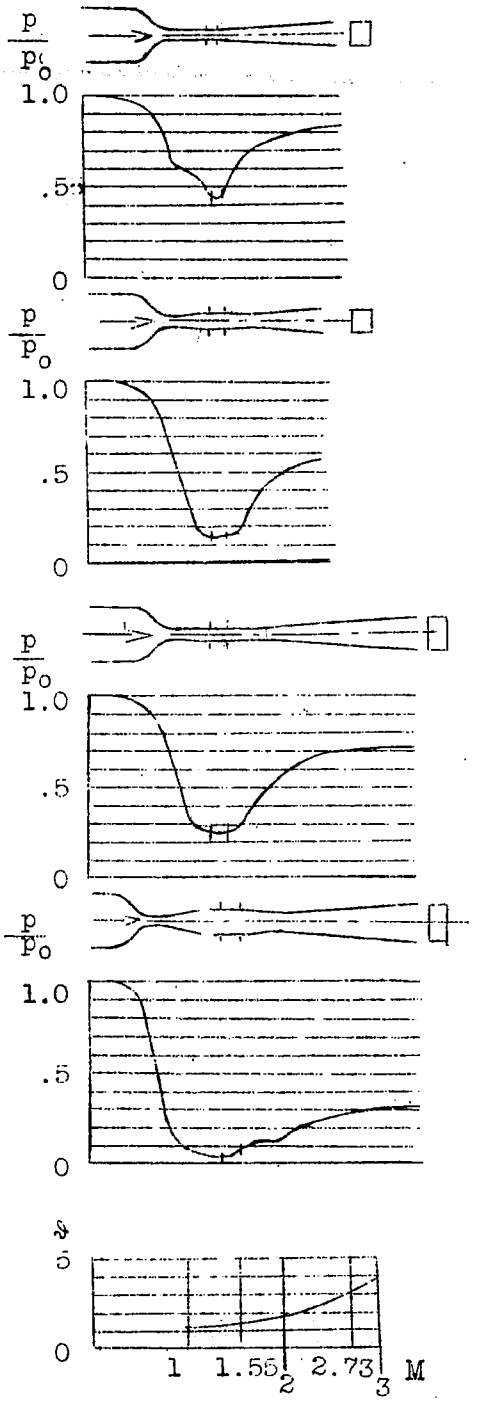

Figure 31.- Diffusor tests for supersonic wind tunnel. Blower pressure ratio θ as a function of the Mach number M.

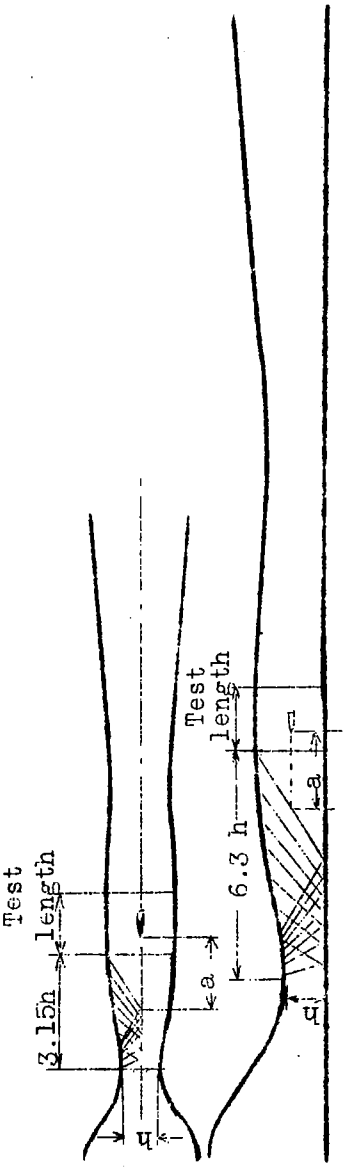

Figure 33.- Supersonic tunnel with movable walls.

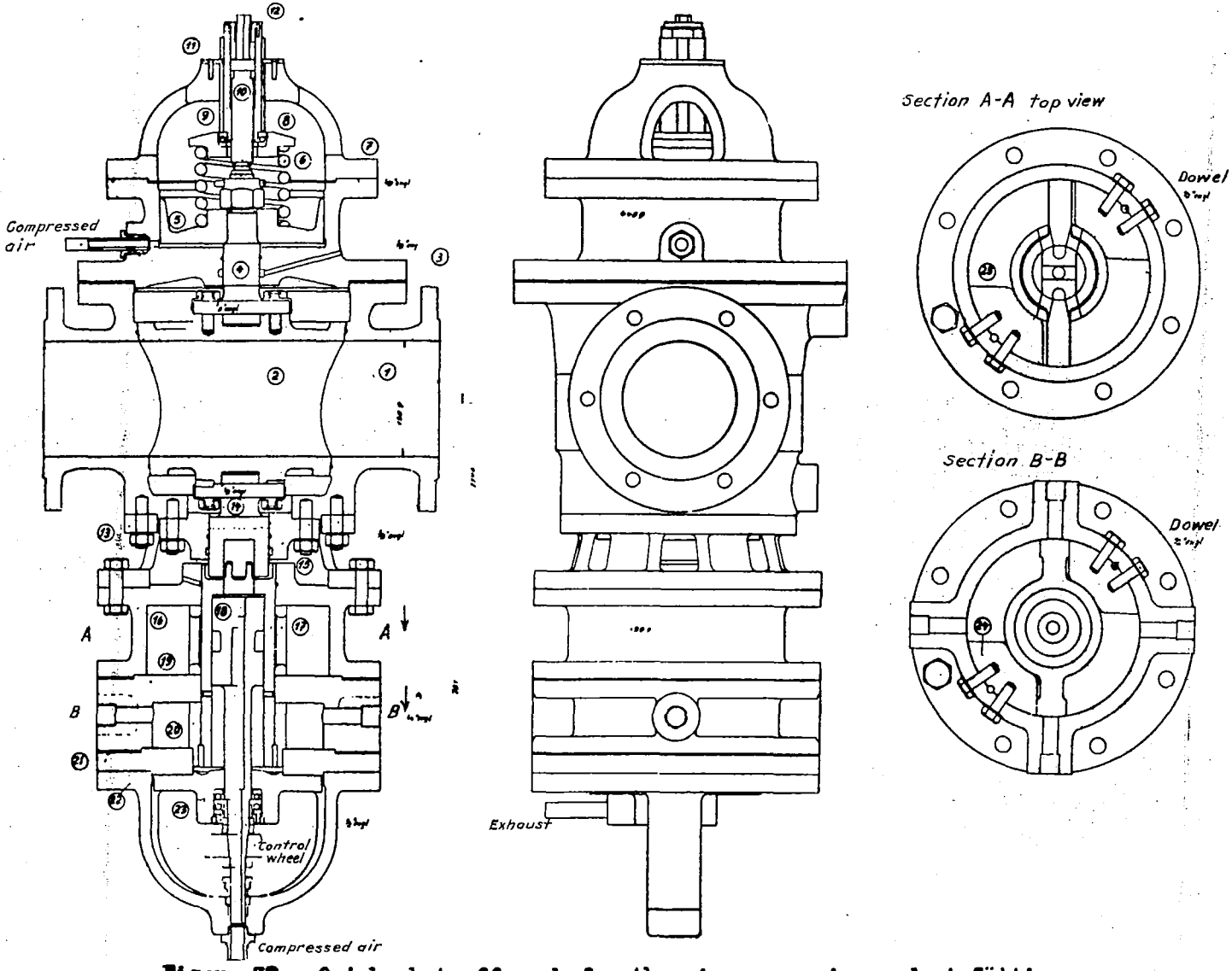

Figure 32.- Quick shut-off cock for the air reservoir, used at Göttingen, operated by compressed air.

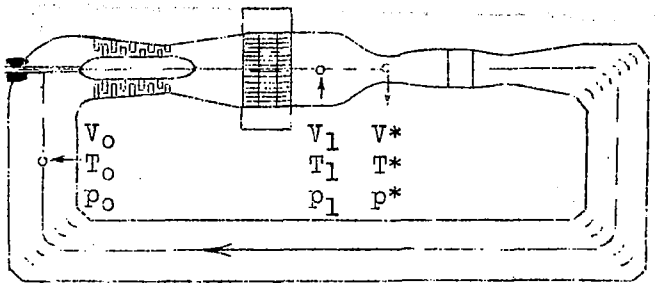

Figure 34.- Sketch for the computation of the test section.

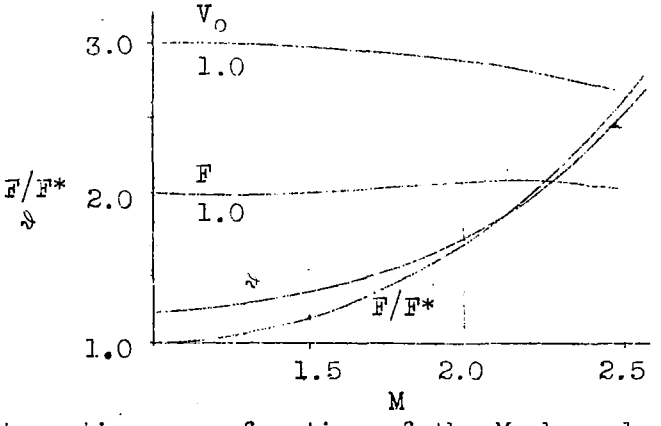

Figure 35.- Test section as a function of the Mach number.

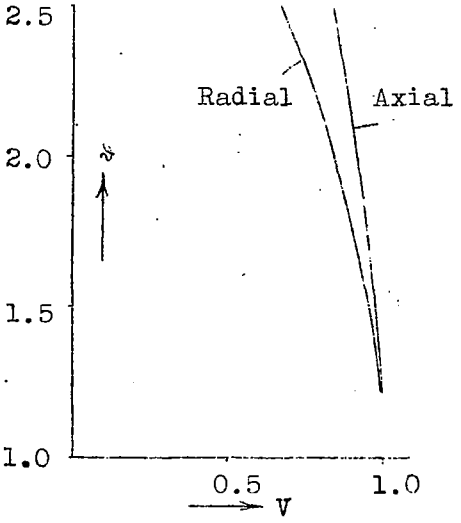

Figure 36.- Comparison of pressure volume characteristics of radial and axial compressors.

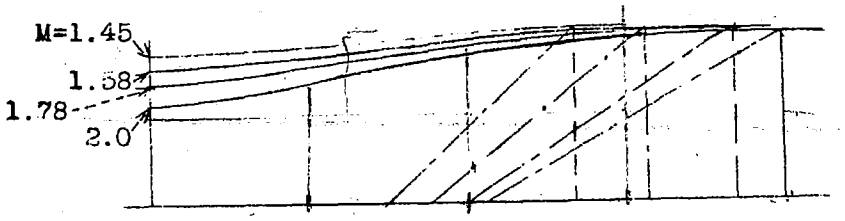

Figure 38.- Nozzle walls for different Mach numbers.

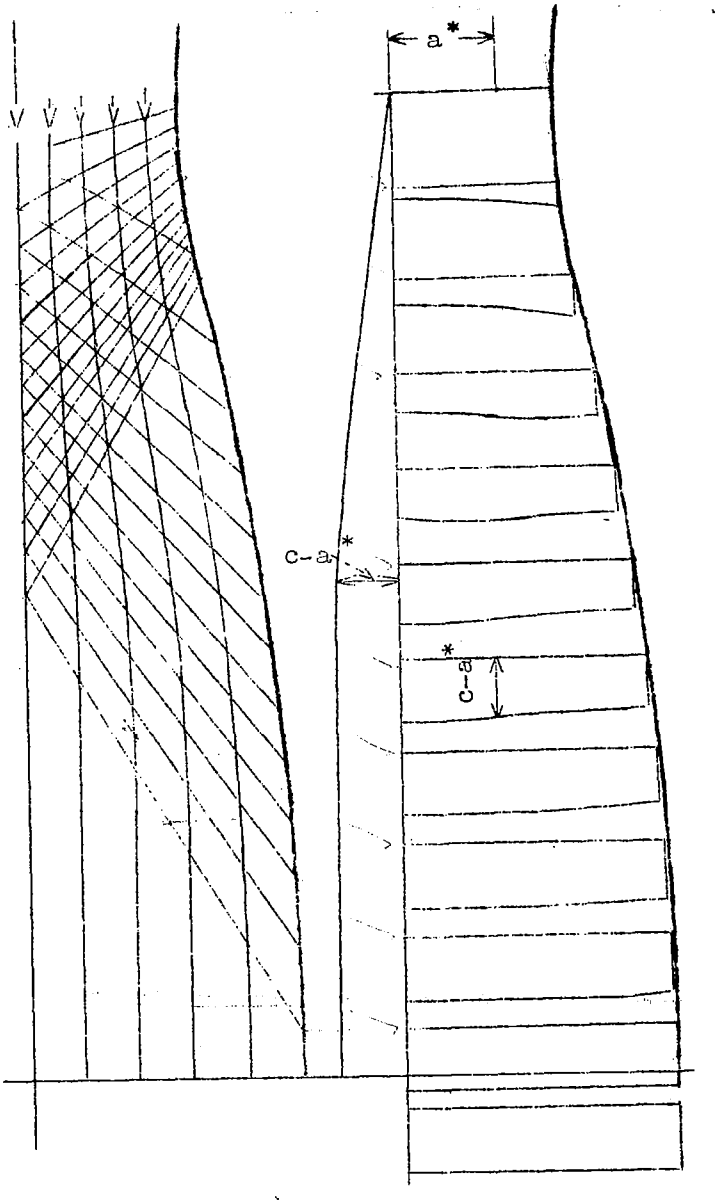

Figure 37.- Laval nozzle drawn by the graphical method of Prandtl-Busemann.

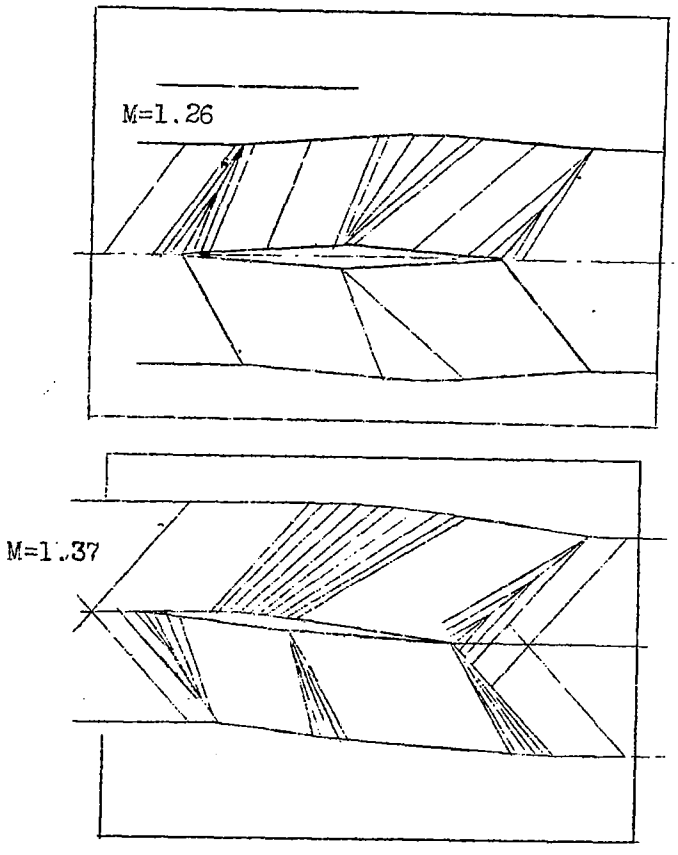

Figure 39.- Shaping the tunnel walls to conform to the flow.

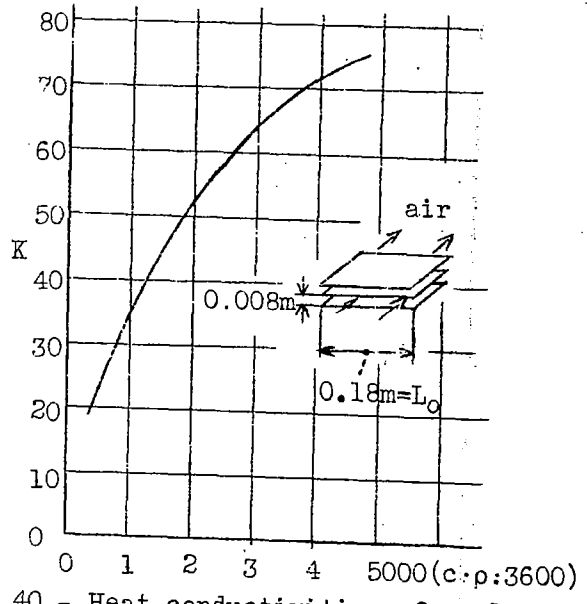

Figure 40.- Heat conductivities of cooler plates.

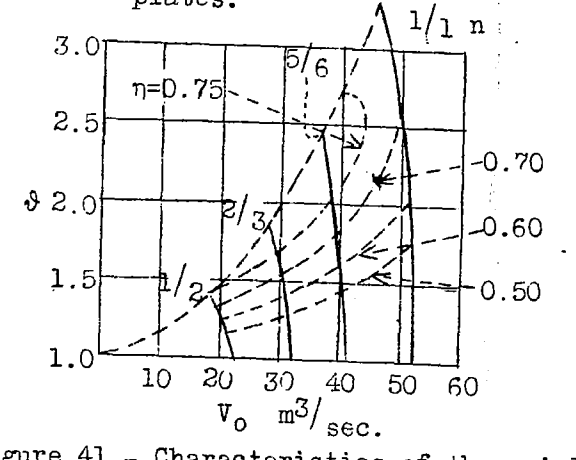

Figure 41.- Characteristics of the axial compressor at the Zürich tunnel.

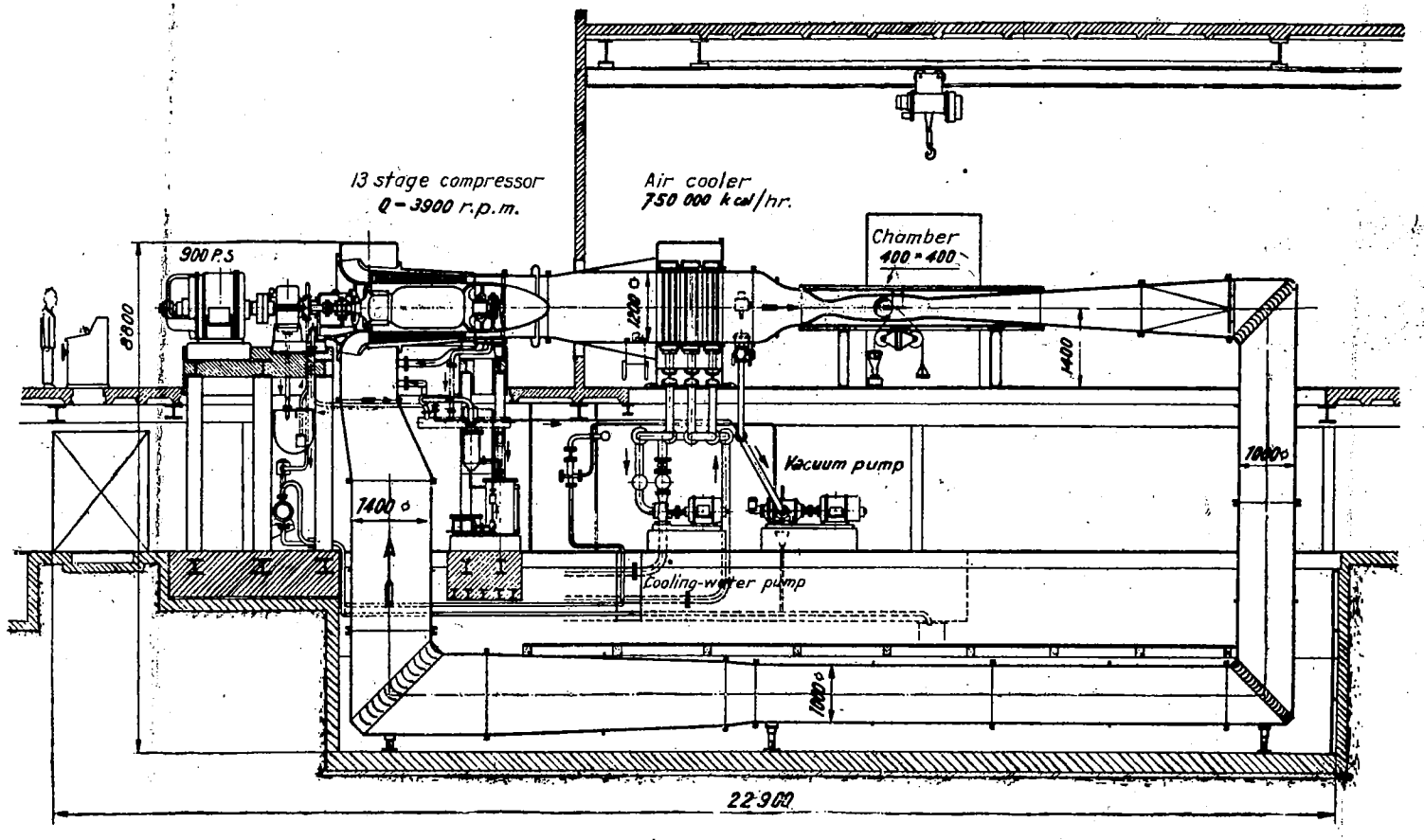

Figure 42.- Section through the supersonic wind tunnel at Zürich.

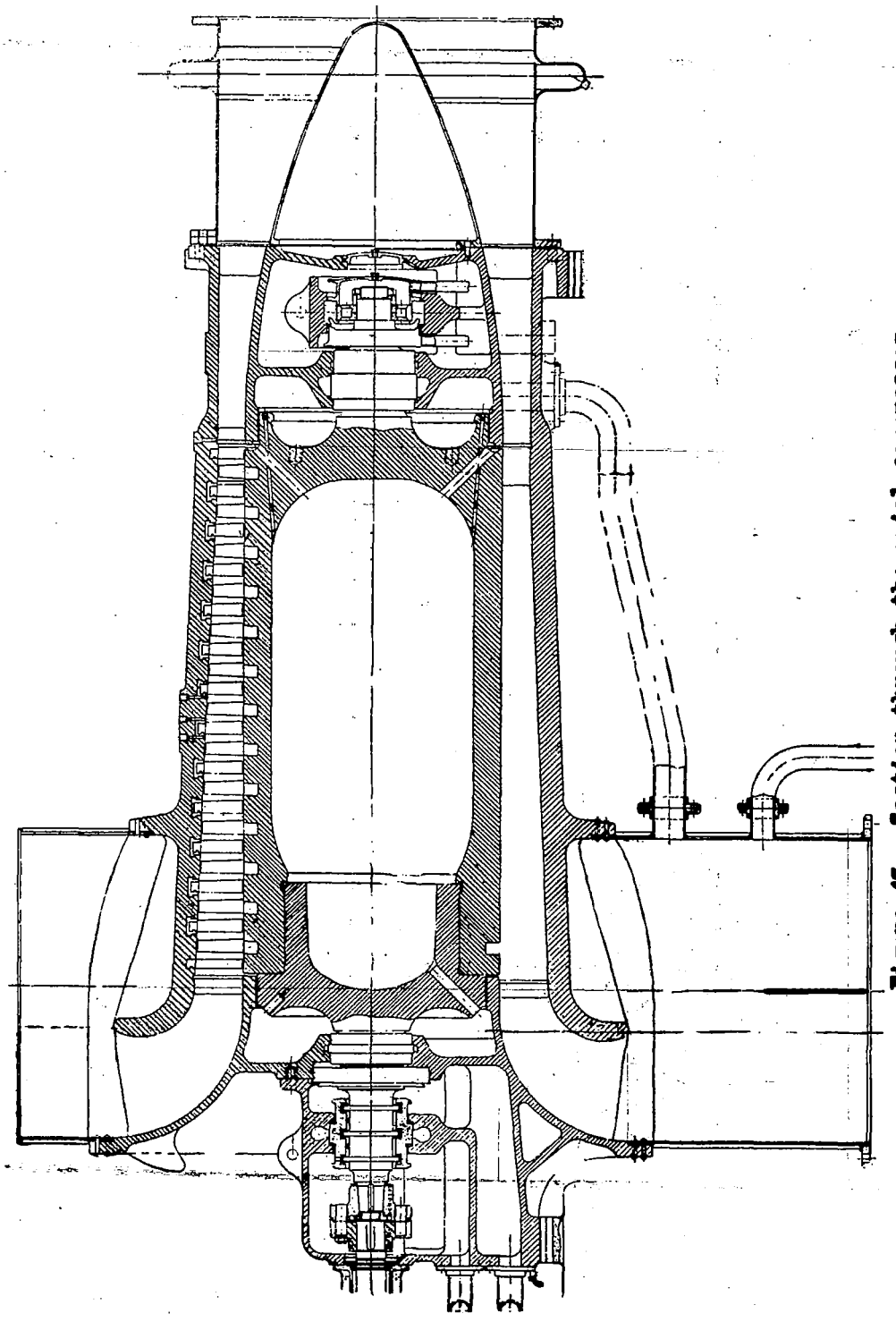

Figure 43.- Section through the axial compressor.

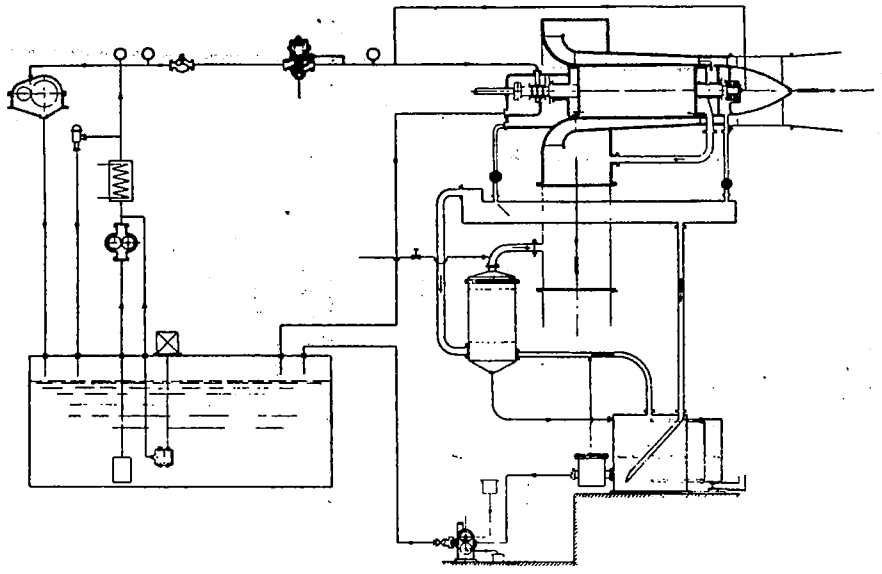

Figure 44.- Oil circulation and oil sealing.

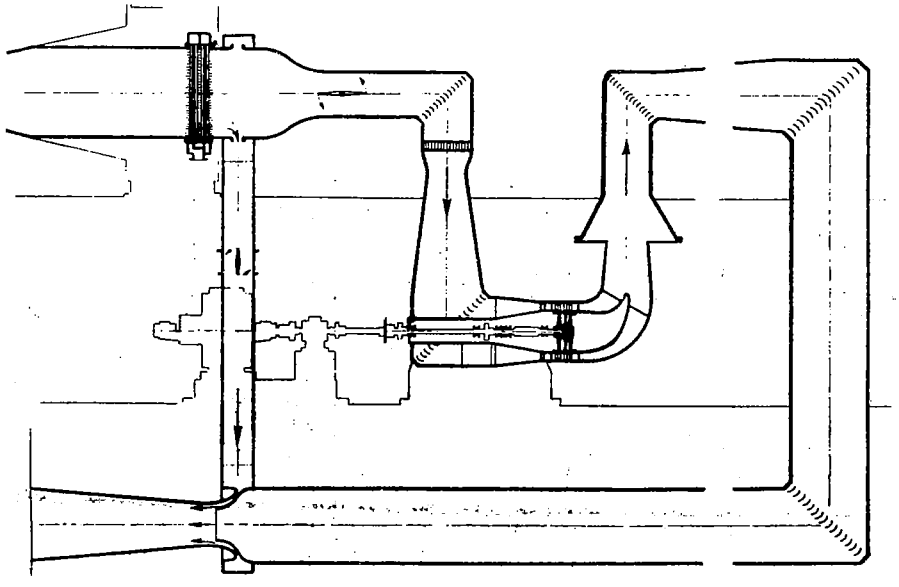

Figure 47.- Installation of the air turbine at the supersonic wind tunnel at Zürich.

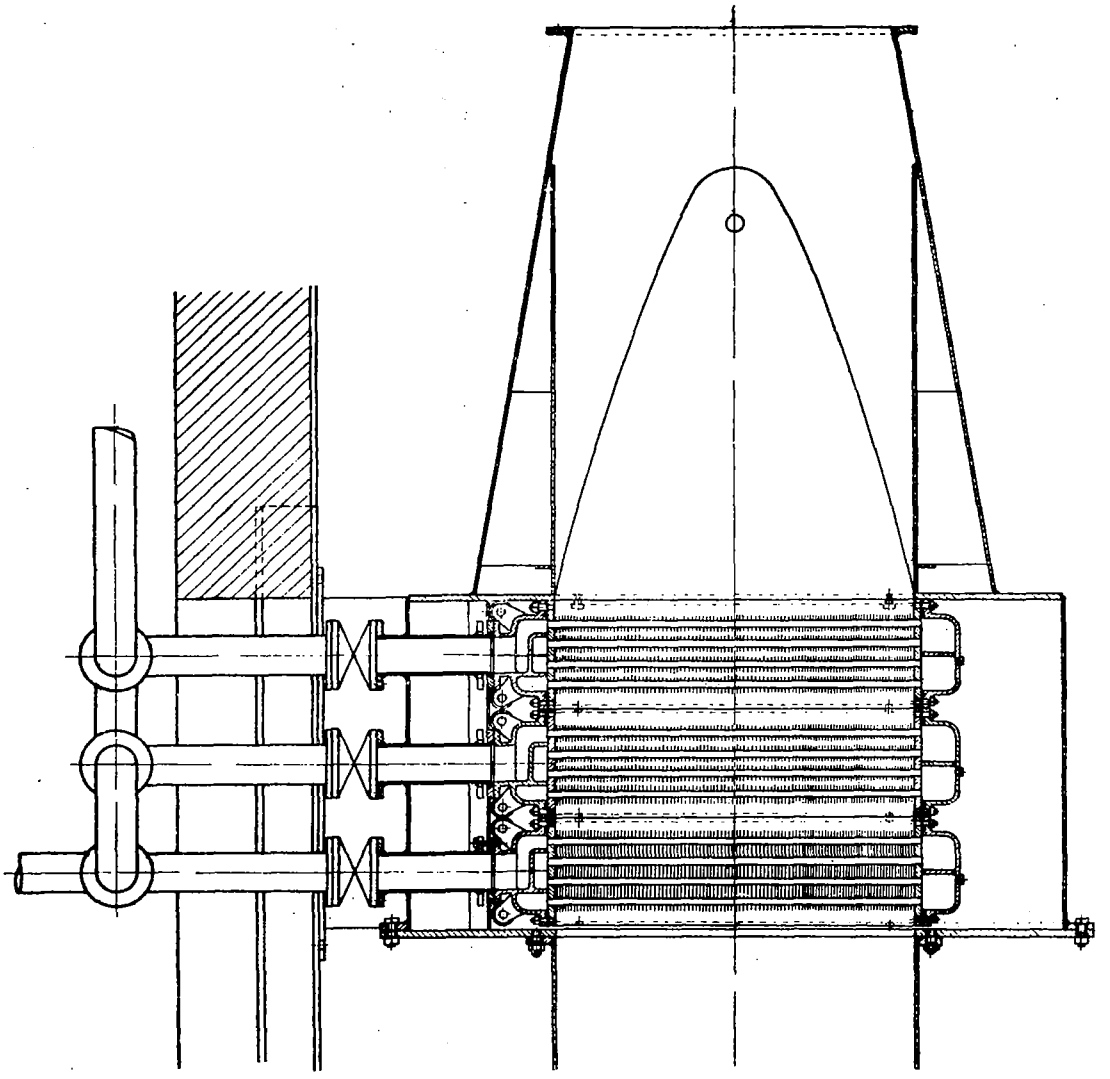

Figure 45.- Cooler having three elements.

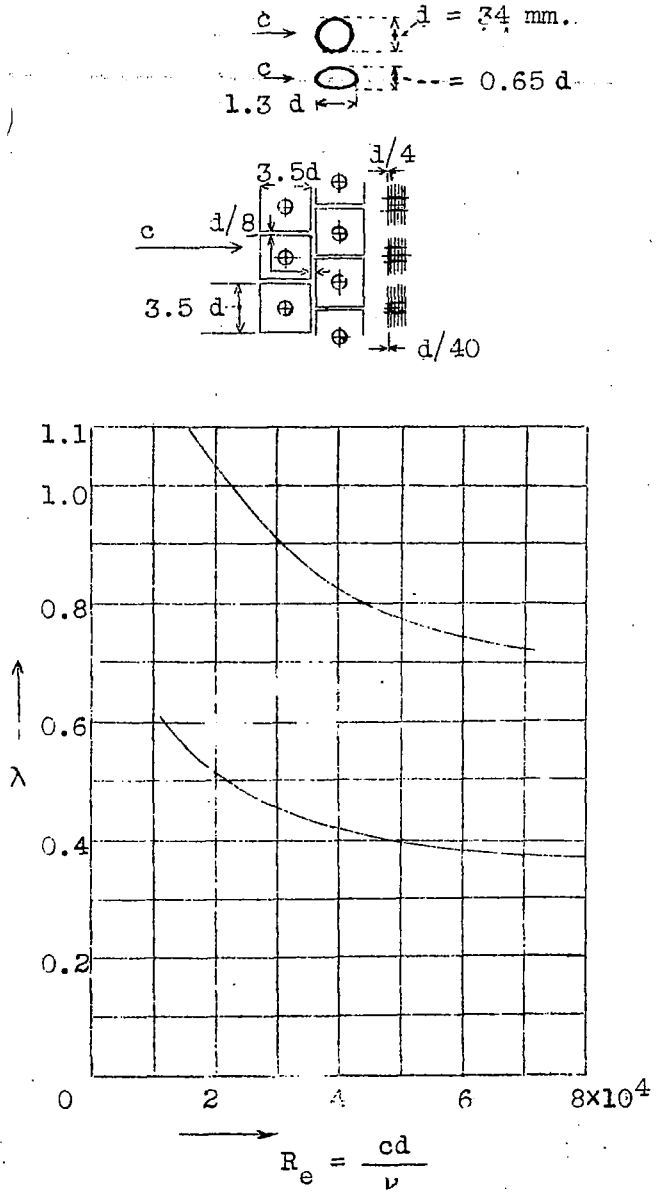

Figure 46.- Reducing the resistance of the cooler by streamlining the cooler pipes.